รายงานวิจัยฉบับสมบูรณ์

โครงการ การประยุกต์ differential scanning calorimetry เพื่อใช้วิเคราะห์ความพรุนของพอลิเมอร์ที่ใช้ในทางเภสัชกรรม

ดำรงศักดิ์ ฟ้ารุ่งสาง

กรกฎาคม พ.ศ. 2550

สัญญาเลขที่ RMU4880025

รายงานวิจัยฉบับสมบูรณ์

โครงการ การประยุกต์ differential scanning calorimetry เพื่อใช้วิเคราะห์ความพรุนของพอลิเมอร์ที่ใช้ในทางเภสัชกรรม

ดำรงศักดิ์ ฟ้ารุ่งสาง
ภาควิชาเทคโนโลยีเภสัชกรรม
คณะเภสัชศาสตร์ มหาวิทยาลัยสงขลานครินทร์

สนับสนุนโดยสำนักงานคณะกรรมการการอุดมศึกษา
และสำนักงานกองทุนสนับสนุนการวิจัย

Executive Summary

โครงการวิจัยนี้ เป็นการวิเคราะห์เชิงความร้อนโดยใช้ differential scanning calorimetry เพื่อศึกษาพฤติกรรมของการเปลี่ยนสถานะระหว่างน้ำและน้ำแข็งที่ปรากฏอยู่กับพอลิเมอร์ที่ใช้ทางเภสัช-กรรม ด้วยน้ำในเมทริกซ์ของพอลิเมอร์ประเภทนี้ มีจุดเยือกแข็งลดต่ำลง อาจเนื่องมาจากน้ำแข็งถูกกักในรูพรุนของพอลิเมอร์หรืออันตรกิริยาระหว่างน้ำและพอลิเมอร์เอง ซึ่งทั้งสองทฤษฎีต่างก็มีงานวิจัยสนับสนุน แต่ไม่เคยมีงานวิจัยใดที่ประยุกต์ทั้งสองทฤษฎีกับการทดลองที่มี setting เดียวกันเลย งานวิจัยชิ้นนี้ มีสมมติฐานว่า ปรากฏการณ์ที่เกิดขึ้นในระบบพอลิเมอร์-น้ำ นี้เป็นไปได้ทั้ง 2 ทาง ขึ้นอยู่กับสัดส่วนปริมาณน้ำที่อยู่ร่วม พบว่า ที่ความชื้นสัมพัทธ์ไม่สูงมากนัก น้ำเริ่มทำอันตรกิริยาจำเพาะกับพอลิเมอร์ ณ ส่วน hydrophilic ของพอลิเมอร์ และ ด้วยคุณสมบัติทางพันธะไฮโดรเจนของน้ำ เมื่อความชื้นสัมพัทธ์สูงขึ้น น้ำจะปกคลุมพื้นผิวของพอลิเมอร์และควบแน่นในรูพรุนของพื้นผิว อย่างไรก็ตาม ในสภาพแวดล้อมที่มีน้ำมากเกินพอ ระบบพยายามลดพลังงานอิสระที่ผิว (surface free energy) ลง น้ำแข็งในรูพรุนจึงเปลี่ยนสถานะเป็นน้ำอิสระ (bulk water) แล้วตกเป็นน้ำผลึกอีกครั้งหนึ่ง ทำให้น้ำในสถานะอิสระมีมากขึ้น อีกทั้งโครงร่างพอลิเมอร์ที่ประกอบเป็นรูพรุนมีการขยายและคลายตัวออก ทำให้พฤติกรรมละลายในน้ำของพอลิเมอร์เด่นชัดขึ้น ทั้งนี้ขึ้นกับความสามารถในการละลายน้ำของพลิเมอร์เอง งานวิจัยชิ้นนี้ได้ประยุกต์ใช้แบบจำลองทั้ง 2 ทฤษฎี กับ พอลิเมอร์ที่ใช้ทางเภสัชกรรมประเภทคาร์โบไฮเดรท ได้แก่ โซเดียมแอลจิเนท แป้งโซเดียมไกลโคเลท แป้งมันสำปะหลังพร้อมก่อเจล รวมทั้งอนุพันธ์ของเซลลูโลส ได้แก่ ไฮดรอกซีโปรปิวเมทิลเซลลูโลส โซเดียมคาร์บอกซีเมทิลเซลลูโลส และ ครอสอะเมลโลสโซเดียม ได้อย่างสำเร็จ พบว่ารูพรุนที่บรรจุน้ำ (hydro-pores) ในขณะพอลิเมอร์อยู่ในรูปเจล มีขนาดพอๆกับส่วนของรูพรุนขนาดกลางของพื้นผิวพอลิเมอร์ที่ได้จากการวัดโดยเทคนิกการดูดซับไนโตรเจนบนพื้นผิว ซึ่ง hydro-pores ดังกล่าว น่าจะสะท้อนสภาพเป็นจริง และ มีบทบาทสำคัญในการปลดปล่อยยาผ่าน hydrogel ในระบบนำส่งยา (drug delivery system).

บทคัดย่อ

ในเมทริกซ์ของพอลิเมอร์และน้ำ จุดเยือกแข็งของน้ำลดต่ำลงอาจเนื่องมาจากน้ำแข็งถูกกักในรูพรุนของพอลิเมอร์หรืออันตรกิริยาระหว่างน้ำและพอลิเมอร์ วัตถุประสงค์ของงานวิจัยชิ้นนี้ ได้แก่ การศึกษากระบวนการลดจุดเยือกแข็ง / หลอมเลวของน้ำแข็งดังกล่าวโดย ดิฟเฟอร์เรนเชี่ยล สแกนนิ่ง แครอริมิเตอร์อุณหภูมิต่ำ (sub-ambient DSC) พอลิเมอร์ทางเภสัชกรรมที่ใช้ศึกษา ประกอบด้วย พอลิแซคคารายด์ ได้แก่ โซเดียมแอลจิเนท (SA) แป้งโซเดียมไกลโคเลท (SSG) แป้งมันสำปะหลังพร้อมก่อเจล (PS) รวมทั้งอนุพันธ์ของเซลลูโลส ได้แก่ ไฮดรอกซีโปรปิวเมทิลเซลลูโลส (HPMC) โซเดียมคาร์บอกซีเมทิลเซลลูโลส (SCMC) และ ครอสอะเมลโลสโซเดียม (CCS) ศึกษาลักษณะของตัวอย่างโดยกล้องจุลทรรศน์อิเลคตรอนแบบส่องกราด และ เครื่องเลี้ยวเบนรังสีเอกซ์ ใช้การดูดซับไนโตรเจนทำการหาขนาดและการกระจายขนาดรูพรุนระดับกลางบนผิวตัวอย่าง ทำการเตรียมตัวอย่างโดยให้ตัวอย่างอยู่ในบรรยากาศที่มีความชื้นสัมพัทธ์สูง (ความชื้นสัมพัทธ์ร้อยละ 85-100 ณ อุณหภูมิ 30.0$\pm$0.2° ซ 10 วัน) และผสมกับน้ำปริมาณมากเกินพอ (hydrogels) จากนั้น วิเคราะห์ตัวอย่างด้วย sub-ambient DSC วงจรอุณหภูมิ ระหว่าง 25 และ -150 ° ซ ที่ อัตราเร็ว 5.00° ซ/นาที วัดสัดส่วนปริมาตรของตัวอย่าง hydrogels โดยเทคนิคการกระเจิงของแสง และ วัดระดับความชื้นในตัวอย่างโดยเครื่องชั่งความชื้น พบว่าพอลิเมอร์ตัวอย่างที่ศึกษาส่วนใหญ่อยู่ในรูปอสัญฐาน ณ บรรยากาศความชื้นสัมพัทธ์สูง น้ำที่อยู่ด้วยกันกับตัวอย่างทั้งหมดยกเว้น PS และ HPMC สามารถเยือกแข็งได้ 2 ส่วน ได้แก่ ที่อุณหภูมิที่ต่ำกว่าจุดเยือกแข็งปกติ (bound water) และ ที่จุดเยือกแข็งปกติ (bulk water) การลดลงของจุดเยือกแข็งของ bound water อาจเป็นเพราะอันตรกิริยาจำเพาะระหว่างน้ำและพอลิเมอร์ตามแบบจำลองของ Flory หรือ น้ำถูกกักอยู่ในโครงร่างพอลิเมอร์ซึ่งเป็นไปตามผลของ Gibb-Thomson สารละลายพอลิเมอร์ตามแบบจำลองของ Flory สามารถประยุกต์เข้ากับข้อมูลสัดส่วนปริมาตรและอุณหภูมิหลอมเหลวที่ได้จากสัญญาณ DSC ของตัวอย่าง hydrogels ได้อย่างเป็นผลสำเร็จ โดยพบพารามิเตอร์อันตรกิริยาของ Flory (χ_1) ระหว่าง 0.520 และ 0.847 สังเกตได้ว่า χ_1 ยิ่งต่ำ อุณหภูมิเยือกแข็งของ bound water ยิ่งลดลง กล่าวคือ อันตรกิริยาสำหรับน้ำยิ่งแข็งแรง การวิเคราะห์รูปร่างสัญญาณ DSC ของ bound water โดยคอมพิวเตอร์ ทำให้สามารถแยก bound water บนผิวของ SA และ SSG ในบรรยากาศความชื้นสัมพัทธ์สูงออกเป็น 2 ส่วน ได้แก่ ส่วนที่เกี่ยวกับอันตรกิริยาระหว่างพอลิเมอร์และน้ำ และ ส่วนที่ถูกกักอยู่ในรูพรุนซึ่งสามารถวิเคราะห์ความพรุนแบบความร้อนได้สำเร็จ โดยได้รัศมีเฉลี่ย $\pm$ ส่วนเบี่ยงเบนมาตรฐานของ hydro-pores สำหรับ ตัวอย่าง hydrogels ของ SA และ SSG เท่ากับ 17.19$\pm$0.39 และ 13.03$\pm$0.54 นาโนเมตร ตามลำดับซึ่งขนาดดังกล่าวสามารถเทียบเคียงได้กับรูพรุนบนผิวขนาดกลางที่วัดได้จากการดูดซับแก๊สไนโตรเจน ขนาดของ hydro-pores อาจเป็นองค์ประกอบที่สำคัญสำหรับการควบคุมการปลดปล่อยตัวยาผ่าน hydrogel โดยเฉพาะอย่างยิ่งสำหรับยาที่มีโมเลกุลขนาดใหญ่

Abstract

In a polymer-water matrix, freezable water is depressed due to either porosity confinement or interaction. The aim of the study was to examine water crystallization / melting depression by sub-ambient differential scanning calorimetry. Polysaccharides including sodium alginate (SA), sodium starch glycolate (SSG), and pregelatinzed potato starch (PS) as well as cellulose derivatives including hydroxypropylmethyl cellulose (HPMC), sodium carboxymethyl cellulose (SCMC), and croscarmellose sodium (CCS) were employed. The morphology of dry samples was examined using the electron scanning microscopy and the powdered X-ray diffractometry. Mesopore size distribution for each of the samples was determined by nitrogen adsorption. The pre-treated with ambient humidity (85-100% relative humidity, at 30.0±0.2°C for 10 days) and with water in excess (hydrogels) samples were subjected to a cycle of 25 - -150°C-cooling-heating at 5.00 °C/min rate. The volume fractions of hydrogels were measured by light scattering technique and the equilibrium moisture contents of samples were determined using a moisture balance. It was found that the major portion of polymeric materials under study was amorphous. All samples but PS and HPMC with ambient humidity as well as water in excess presented freezable water in two distinct fractions namely bound water where crystallizing / melting temperature was depressed and bulk water. It was postulated that the melting point depression of bound water on polymer surfaces may be either due to the specific interaction between water and functional sites on

polymeric chains modeled by Flory or water held within hydro-pores in structural network formed by swollen polymers which its melting point being depressed by Gibbs-Thomson effect. The volume fraction-melting temperature data derived from endotherms of hydrogels were successfully fitted to Flory's model. The Flory's interaction parameters (χ_1) were found to vary between 0.520 and 0.847. It was observed that the smaller the value of χ_1, the larger melting was depressed, i.e., stronger affinity for water. With the aid of in-house computer software for shape analysis, the bound water fraction on the surfaces of SA and SSG equilibrated with ambient humidity could be separated to 2 sub-peaks, i.e., the minor and major ones corresponded to the interaction and pore confinement, respectively. Thermoporometry was successfully applied to the latter peak. The hydro-pore radii expressed as geometric means $\pm$ standard deviations of SA and SSG hydrogels was estimated to be 17.19$\pm$0.39 nm and 13.03$\pm$0.54 nm, respectively which were comparable with what were determined by nitrogen adsorption. It is suggested that the hydro-pore radii may be an important factor when it comes to hydrogel control release of the drug especially in a large molecular size.

Table of Content

List of Tables

List of Figures

Introduction

The interactions of water with pharmaceutical solids are of vital importance for a number of reasons such as the stability (physical, chemical, and biological) and the release of drugs. The chemical nature of an excipient plays an important rule in water sorption since it may, more or less, draw water into the dosage. Starch and cellulose based materials derived from naturally occur biopolymers are the major pharmaceutical excipients utilized in drug delivery dosage forms. This study is dealing with a number of those biopolymers including carbohydrate and its derivative as well as cellulose derivatives. Usually, starch is a mixture of polymers consisting of α-D-glucose as the monomeric unit. There exist two types of starch polymers, i.e., amylose and amylopectin referring to linear and branched polymers, respectively. Most of the morphological structure of a starch polymer exists as an amorphous form. Very dry starches exhibit little crystallinity (about 15-39% for native starches (Levine and Slade, 1988)). Potato starch appears as nearly spherical granules with average diameter of about 10-15 μm**.** Sodium starch glycolate is a low-substituted derivative of potato starch, commercially available under the trade name of Explotab (FMC Corp. USA), obtained by cross-linking and carboxymethylating. Approximately 25 carboxymethyl groups are introduced for every 100 glucose units. Sodium alginate which is the sodium salt of alginic acid is polyelectrolyte carbohydrate. It is a copolymer consisting of β-D-mannuronate and its C-5 epimer α-L-guluronate derived from seaweed and sometime produced by bacteria. The sequence of this copolymer is always random so that amorphous form mainly presents. And,

cellulose is a linear polymer consisting of anhydroglucose units connected together by 1, 4-β-glucosidic linkages. The long polymer chains are made of crystalline and amorphous regions. X-ray diffraction studies revealed that the crystalline regions had lengths of about 600 Angstroms and widths in the range of 50-150 Angstroms (Zografi and Kontny, 1986). Carboxymethyl cellulose is the cellulose ether produced by reacting alkali cellulose with sodium monochloracetate in a slurry system. It is made to undergo an internal cross-linking reaction by lowering the pH of the solution, followed by heating without adding any chemical additive to produce the cross-linked product commercially available as Ac-di- sol (croscarmellose sodium, FMC Crop.).

Carbohydrates and celluloses always interact with water due to their hydrophilicity exhibiting some properties that may critically affect the dosage form performance. It has been revealed that in low range of relative humidity the adsorption occurred only on the hydrophilic sites namely surface hydroxyls and was mainly due to the hydrogen bonding (Sair and Fetzer, 1944) .At increasing relative humidity, the adsorption became appreciable on hydrophobic parts of the surfaces. At very high relative humidity, the distinction between hydrophobic and hydrophilic surfaces disappeared. Earlier investigators (Sair and Fetzer, 1944) suggested at least two forms of sorbed water, i.e., adsorption and capillary water, presented on the starches and celluloses surfaces. With liquid water in excess, starches, celluloses, and their derivatives may form hydrogels, i.e., the three-dimensional arrangement possessing the ability to retain a significant fraction of

water without complete dissolving. Hydrogel might form relatively stable space lattice or pores fulfilled with a significant amount of water which may be considered earlier as capillary water. The interfacial tension related to surface of curvature of water within pores could develop and affect the phase transition of the water. Thus this phase transition of water confinement could somehow characterize the pores where it occupies. A number of authors, for examples: Yamamoto at al. (2005), Faroongsarng and Peck (2003), Hay and Laity (2000), and Ishikiriyama and Todoki (1995) examined the pore sizes and distributions of various porous materials assuming that water is mostly held within pores, with melting temperature being depressed by Gibbs-Thomson effect. However, the depression of melting temperature is not only attributed by water confinement in porosity but the water-polymer interaction. Rault et al (1994) reported that the melting depression and the concentration of unfrozen water varied with the water concentration with similar orders of magnitude for polymer-water systems and simple binary mixtures, presenting the same type of interaction, from which confinement effects are absent. They concluded that the melting depression is due not to water confinement in polymer network but rather to water-polymer interaction. The evidence was later emphasized by the work of Okoroafor et al (1998).

It has been later proposed (Ping, et al. 2001; Zografi and Kontny 1986; and Higuchi and Iijima 1985) that water in hydrophilic polymer matrices presents in three distinct fractions: (i) non-freezable bound water, (ii) freezable bound water,

and (iii) free or bulk water. Upon cooling, water begins to crystallize only when its content is above a characteristic threshold. This fraction of water has been called freezable bound water (fraction (ii)) because it exhibits a melting point lower than zero °C which is distinguished from bulk water and it should correspond to the depression phenomenon described above. In the lower-than-threshold level, i.e., the water of fraction (i), the molecules of water interact with polar functional groups such as carboxyl groups on polymer chains. The interaction would be well-oriented hydrogen bonding which is locally favorable configuration that being strong enough to prevent water to form ice crystals (Ping, et al. 2001). The differential scanning calorimetric (DSC) study can reveal only water of fractions (ii) and (iii). For example: Nakamura et al. (1981) reported two DSC peaks of crystallization of absorbed water on celluloses including a broad peak observed at ~ 230-250 K and a sharp one at ~ 255 K. Should the melting depression of water of fraction (ii) be due to polymer-water interaction, the corresponding DSC peak then could describe the thermodynamics of a polymer in aqueous solution. Although many techniques are available for the experimental determination of the interaction parameter between solvent molecules and the polymeric chain segment such as vapor sorption and laser light scattering methods (Mantovani, et al., 2000), non has been directly done by DSC melting/freezing depression. The aim of the study is to examine the thermal behavior of water melting depression when present with the selected carbohydrate and cellulose based polymers commonly used in drug delivery formulations by mean of DSC technique.

Materials and Method

Carbohydrate and cellulose polymers

The variety in nature of carbohydrate and cellulose based polymers including pre-gelatinized potato starch (PS: Starch®1500, Colorcon, Inc., PA, USA), sodium alginate (SA: Wendt-Chemie, Hamburg, Germany), sodium starch glycolate (SSG: Explotab®, JRS Pharma, Rosenberg, Germany), hydroxypropyl methyl cellulose (HPMC: Colorcon, Inc., PA, USA), Sodium carboxymethyl cellolose (SCMC: Wendt-Chemie, Hamburg, Germany) and croscarmellose sodium (CCS: Ac-di-sol®, FMC Corp. PA, USA) were employed. SA, PS, and SSG were charged-linear, branch and linear, and charged-crosslinked polysaccharides, respectively. HPMC, SCMC, and CCS were linear, charged-linear, and charged-crosslinked celluloses, respectively.

Material morphology studies

The microscopic morphology of the various samples was examined by electron microscope (JSM-5800LV, Jeol SEM, Jeol Technics Company Ltd., Tokyo, Japan). A sample was mounted and coated with gold-platinum to increase the conductivity of surface prior to examination. Photomicrographs with magnified powers of X500, X2,000, and X7,000 of each of the samples were taken.

To examine the crystalline structure, the samples were subjected to powdered X-ray diffraction. The pressed powdered samples were placed in the diffractometer with X-ray radiation emitting Cu tube (Philips X'Pert MPD, Royal

Philips Electronics, Inc., The Netherlands). The angle (2θ) varied between 5 and 90 degrees.

Mesopore analysis by mean of Nitrogen adsorption method

A variety of quantities of nitrogen adsorbed on the dry powder surface of each of the samples at various equilibrium pressures was measured by static volumetric method. In the automatic surface area and pore size analyzer (Coulter SA3100, Beckman Coulter, Inc., Fullerton, CA), the accurately weighed powdered samples were pretreated by evacuation outgasing for 3 hours at 90 °C to remove surface moisture and contaminants. The samples were then placed in the analysis where nitrogen was allowed to be adsorbed on the surface of the powders at five different equilibrium relative pressures up to $(0.03)P/P_0$, at 77 K. The accurate adsorbed nitrogen volume for each relative pressure was measured. The data were derived to adsorption BJH pore volume distribution with the diameter range of 5-160 nm with the aid of the instrument computer software (Coulter SA3100 Version 2.13).

Sub-ambient differential scanning calorimetric study

The Perkin-Elmer differential scanning calorimeter (DSC7 with TAC7/DX Thermal analysis controller, Perkin-Elmer Crop., Norwalk, CT, USA) equipped with liquid nitrogen bath set as a cooling accessory was employed. The 2-point calibrations with Indium and Cyclohexane were carried out for every time which the DSC operation started to ensure the accuracy/precision of the obtained heat of transitions and the corresponding temperatures. The operation was randomly monitored by running an Indium reference standard and it was found that both

temperature and heat of transition deviated from expected values by less than 2.00%.

An accurately weighed (5-15 mg) sample was placed in tightly sealed aluminum pan (Perkin-Elmer Crop., Norwalk, CT, USA).With loading temperature of 25 °C, the analysis program includes 1) cooling from 25 °C to -150 °C at 5.00 °C/min rate, 2) isothermal run at -150 °C for 1 min, and 3) heating from -150 °C to 25 °C at the same rate as cooling step. The summary of DSC conditions is in Table 1.

DSC Parameter	Set condition
Loading temperature	25.00 ^{o}C
Initial heat flow	20 mW
Scanning conditions	
Cooling track	25.00 to -170.00 ^{o}C
Cooling rate	5.00 ^{o}C/min
Holding	-170.00 ^{o}C for 1 min
Heating track	-170.00 to 25 ^{o}C
Heating rate	5.00 ^{o}C/min
Ending condition	25.00 ^{o}C
Calibrations	Cyclohexane, Indium
Sample weight	2-10 mg accurately
DSC pan	Hermetically sealed

Table 1 The conditions utilized for differential scanning calorimetric study (DSC7 Perkin-Elmer Crop., Norwalk, CT, USA)

The distilled water was subjected to the run to validate the temperature and heat of water crystallization / melting. All of DSC thermograms (cooling or heating traces) were analyzed using Pyris software (Perkin-Elmer Perkin-Elmer Crop., Norwalk, CT, USA).

The pre-treated with ambient humidity samples including, PS, SA, SSG, HPMC, SCMC and CCS were subjected to investigation. Prior to DSC analyses, samples were equilibrated with 85, 96, and 100% relative humidity (RH) at

30.0±0.2 °C for 10 days. The samples were also fully hydrated by liquid water in excess at the same temperature as those pre-treated with ambient humidity as follows: A 3- to 8-gram sample (equivalent to approximately 10-ml bulk volume) was thoroughly mixed with liquid water to 100 ml in volume. The mixtures were allowed to be still for 1 day. Hydrogels and/or sediments depending to the nature of water-polymer mixtures were subjected to sub-ambient differential scanning calorimetric study described above. The total water (W_T) contents of hydrogel/sediment samples were determined using a moisture balance (Metter LP16 & PM300, Metter-Toledo, Inc., Hightstown, NJ, USA).

The determination of non-freezable water (*water of fraction (i)*)

The water of fraction (i) was calculated by subtracting the total water content (W_T) by the water content calculated from the amount of heat corresponded to DSC melting traces in sub-ambient temperatures assuming that the heat was directly proportional to molar heat of melting obtained from DSC tracing of distilled water.

The determination of polymer volume fraction in liquid water

The fully hydrated polymer volume fraction (ϕ_{2V}) was obtained from particle size determination in non-swelling and swelling states, as analogous to what was done previously (Mantovani et al., 2000). The size and distribution of each of the polymeric powders were measured by dynamic laser light scattering technique (Mastersizer/E, Malvern Instruments Ltd., Worcestershire, UK). Alcohol and water were used as non-swelling and swelling media, respectively.

ϕ_{2V} was obtained by comparing mean volume diameters according to the equation of $\phi_{2V} = \left[\overline{d_{al}} / \overline{d_w}\right]^3$, where $\overline{d_{al}}$ and $\overline{d_w}$ are geometric mean volume diameters of a powdered polymer in alcohol and in water, respectively.

To quantify the polymer volume fraction during ice-liquid phase transition of water denoted by φ_2, it was assumed that only pure water freezes when cooled to freezing point. φ_2 is thus directly proportional to the cumulative partial area under the endotherm at corresponding T, i.e., $\varphi_2 = \varphi_2^{(i)} - \Lambda \frac{A_T}{P}$. Where, A_T, P, $\varphi_2^{(i)}$, and Λ are the area under the endotherm at temperature T, the total area under the endotherm, the polymer volume fraction with water of fraction (i), and the linear coefficient that makes φ_2 equals φ_{2V} determined by light scattering technique, where A_T equals P, respectively. $\varphi_2^{(i)}$ was approximated from mole fraction of water of fraction (i) ($x_1^{(i)}$) calculated based on the water content of non-freezable water previously described, i.e., $\varphi_2^{(i)} \approx (1 - x_1^{(i)})$. The φ_2 and its corresponding T were non-linearly fitted into Flory's model described in next section using the commercial software (SigmaPlot 2000, SPSS, Inc.).

Results and Discussion

The morphology of dry carbohydrates

The surface morphology of polysaccharides more or less reflects the water sorption. The information of their surface may be necessary. Photomicrographs (SEM) of some of the samples under study were taken. They are in Figure 1. As seen in the figure, the surface of PS is found not to be significantly different from that of SSG. Noted that the white spots on the surface of SSG may be due to sodium chloride crystalline present as an impurity from manufacturing process (Edge et al, 2002). Whereas PS and SSG presented somewhat smooth surface, SA exhibited porosity with a few micrometers in size. It is noted that only the surface porosity and irregularity in the range of micrometers which is corresponded to macropores was observed by SEM whereas the size range of interest would be in mesopores (approximately 2 to 50 nm), i.e., the magnitude for the drug molecules could travel when it comes to release from the drug delivery dosage forms.

Figure 2 illustrated the X-ray diffraction patterns of carbohydrate polymers. It is found that major portion of carbohydrates presented as an amorphous form. In addition, the X-ray diffraction of other polymers under study (data not shown) also similarly exhibited these patterns. Cellulose although exhibit a large portion of crystalline form. But its derivatives such as croscarmellose sodium increasingly present as the amorphous form. As the moisture sorption sites for celluloses have been proposed to being located on the amorphous portions (Adamson, 1990), a considerable amount of water may be expected to present on the surfaces of cellulose derivatives employed in this study.

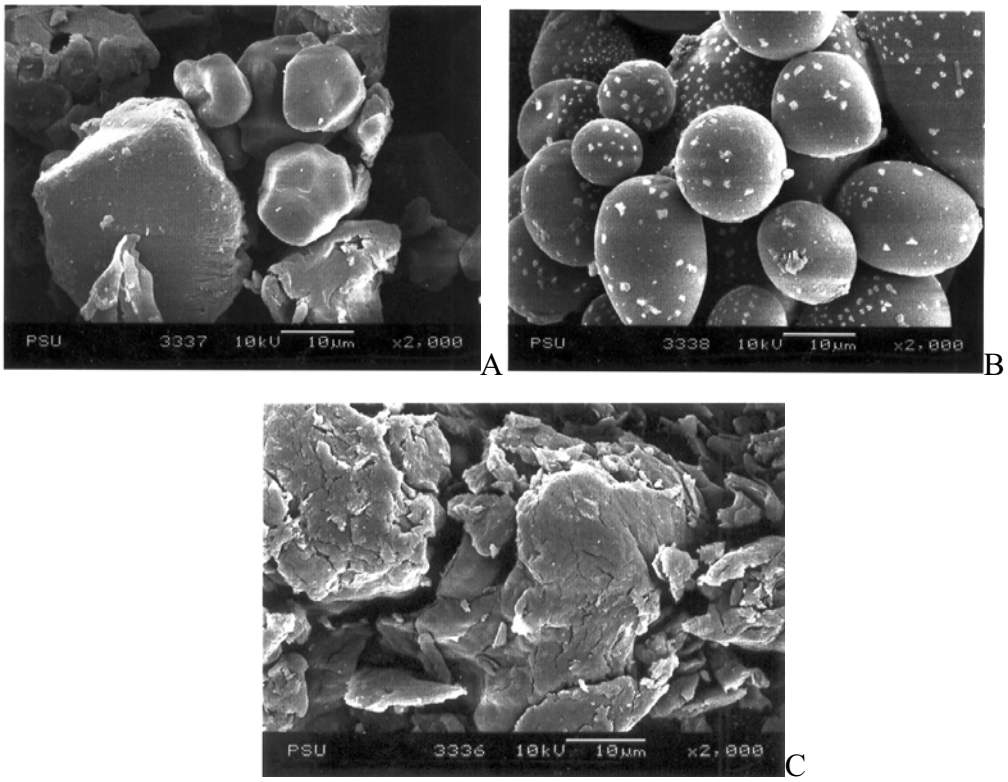

Figure 1 Photomicrographs of Pre-gelatinized potato starch (A), Sodium starch glycolate (B), and Sodium alginate (C) at magnification of X2000

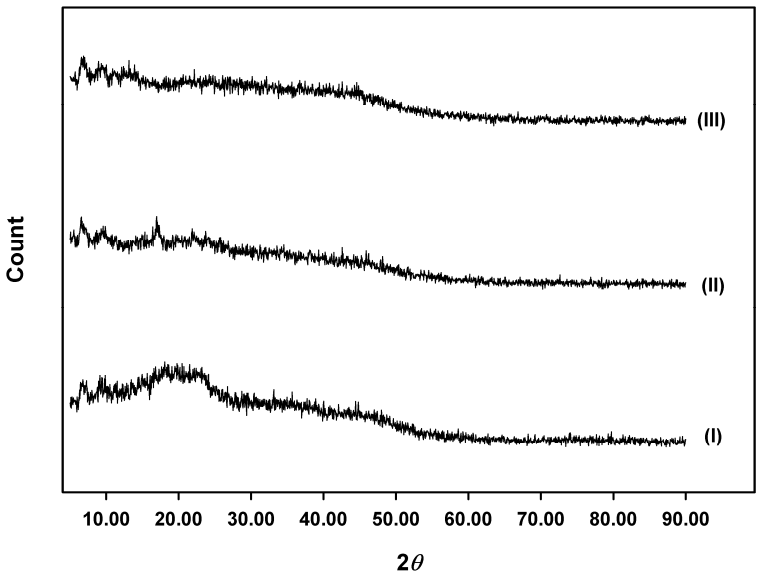

Figure 2 Powdered X-ray diffraction data of carbohydrates polymers including: PS (I), SSG (II), and SA (III).

DSC water tracings of selected hydrophilic polymers in ambient humidity

Figure 3 illustrates the tracings of water that could be found in SA, SSG, SCMC, and CCS equilibrated with ambient humidity (85-100% RH). For simplicity, the only tracings of SA-100%RH system are showed. As seen in Figure 2, the freezable water in current study is consistent with previous report (Nakamura et al., 1981). It is then subjected into 2 fractions, i.e., water of fraction (ii) labeled as (I) where freezing / melting happen at a temperature far below zero, and that of fraction (iii) labeled as (II) where its transitions are closed to normal melting point.

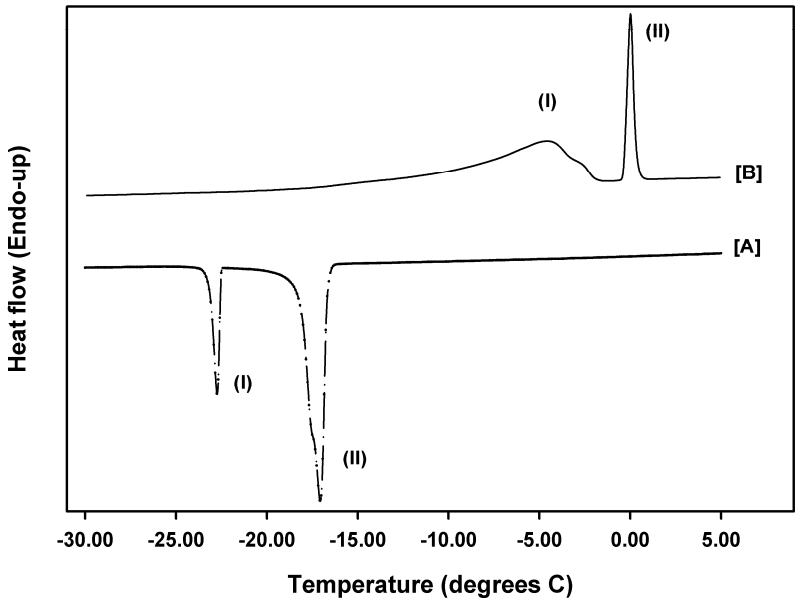

Figure 3 DSC thermograms (cooling [A] and heating [B] curves) of SA previously equilibrated in 100%RH at 30 degrees C for 7 days showing 2 phases of water on polymer surface. (I) is freezable bound water and (II) is bulk water.

Figure 4 compares endothermic traces of water on the 100%-RH-pre-treated PS, SSG, and SA. These three carbohydrate polymers exhibit merely different in terms of water interaction. Unlike SSG and SA, water tracing of PS

presents as the water of fraction (iii) only (Figure 4). Starch has been classified as a moderately hygroscopic material (Callahan et al, 1982) that could absorb moisture up to 20% in ambient humidity. However, the moisture sorption does not exceed the threshold of non-freezable bound moisture content present in starch (28% by weight: Zhong and Sun, 2005).

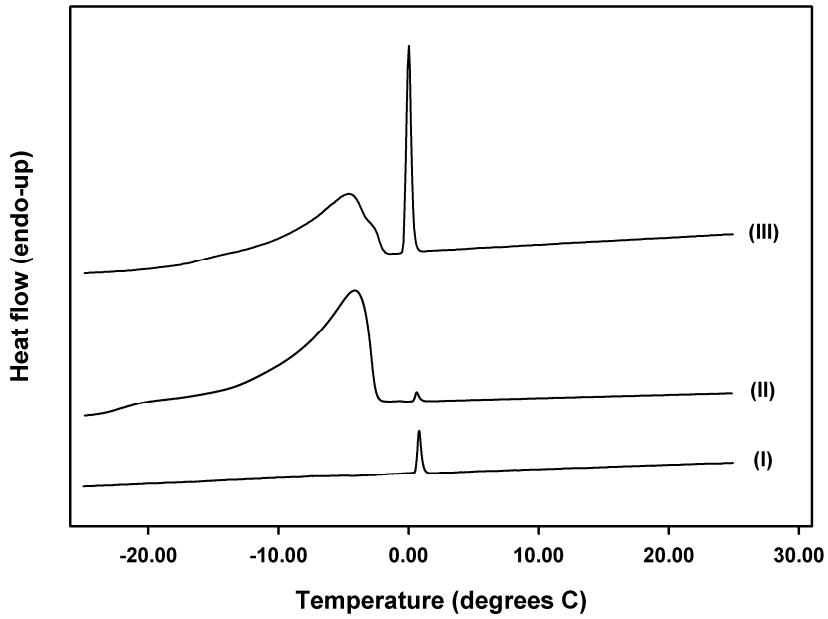

Figure 4 Endotherms of water on 100%RH pre-treated PS (I), SSG (II), SA (III) showing states of freezable water.

The moisture sorption on SA and SSG exceeds the threshold of non-freezable bound moisture content yielding that the water of fraction (ii) could be revealed. Figures 5 and 6 respectively show heating curves of SA and SSG previously equilibrated with various ambient humidity environments. These 2 Figures exhibit the different behavior of water sorption between the two materials. It is observed that the majority of water sorbed on SSG tends to be the water of fraction (ii) while the portions of water of fraction (ii) and (iii) on SA are

approximately equal. SA is water soluble. A significant portion of water may solvate some polymer chains on the surface of SA whereas the rest could interact with specific sites resulting in the approximately equal increased presence of water of fractions (ii) and (iii) with increase in environmental humidity. On the other hand, SSG is non-soluble crosslinked polymers. The water molecules tend to interact with polymer without solvation. The water of fraction (ii) thus increases with increasing environment humidity.

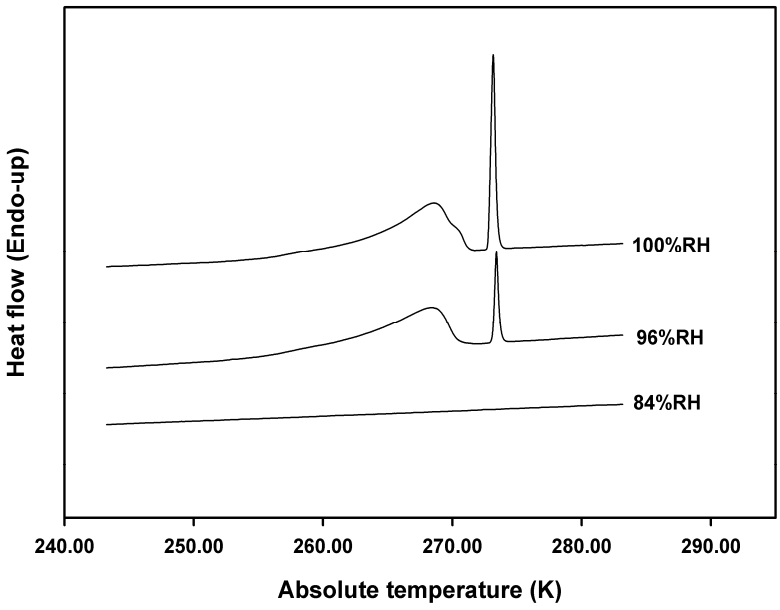

Figure 5 Endotherms of water melting of sodium alginate (SA) pre-treated with various humidity environments (at 30.0+0.5 degrees C for 7 days).

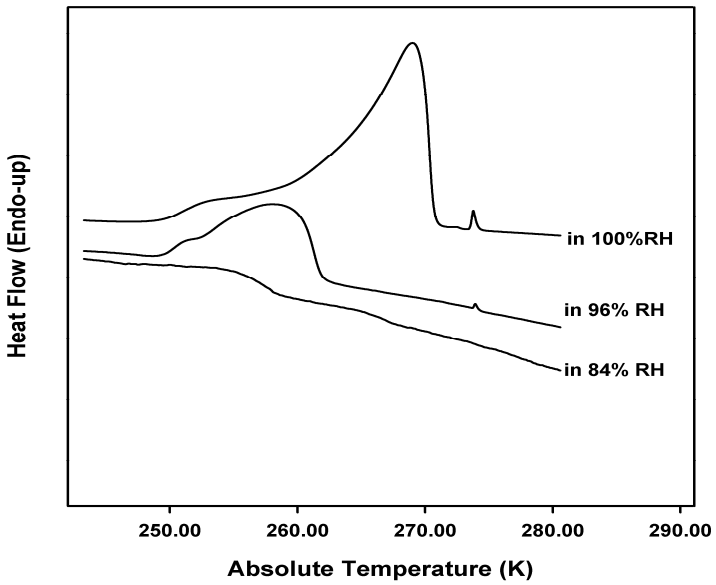

Figure 6 Endotherms of water melting of sodium starch glycolate (SSG) pre-treated with various humidity environments (at 30.0±0.5 degrees C for 7 days).

DSC water tracings of the selected hydrophilic polymers in excess water and the nature of ice-liquid water transition

Figure 7 illustrates the DSC freezing traces of CCS with various aqueous level environments including that with liquid water in excess. It is noted that other polymers in this study showed similar patterns. However, the water transition tracings were absent in the cases of PS and HPMC in ambient humidity but fully hydrated samples. PS and HPMC are non-ionic polymers exhibiting less hygroscopic than others. It may be because ionic species and salts could attribute to water solvation on polymer they present with and might allow amount of water uptake greater than threshold of non-frozen water to show the DSC tracings of water of fraction (ii) and (iii) in cases of SA, SSG, SCMC, and CCS. It is also observed that the phase transition of water of fraction (ii) always exhibits a pattern as a polymer solution, i.e., the more concentration level of water; the more

freezing temperature is depressed. Thus with water in excess, the freezing temperature depression may be treated in accord with polymer-water interaction.

Figure 8 illustrates the endothermic melting traces of SSG with variety of humidity as well as fully hydrated sample. Like freezing exotherms, the melting endotherms of various level of water with polymers under study were also in similar pattern. It is observed that the melting of freezable bound water shifts toward the melting of free water. i.e., the two singlet peaks turn to a doublet with increase in water content which is similar to the previous study (Borchard et al., 2005). It may be because water of fraction (ii), during increasing temperature, becoming liquid phase migrates from the vicinity of polymer interaction sites within gel due to hydrogen bonding among water molecules to be in equilibrium again with free water that melt later at a normal melting temperature.

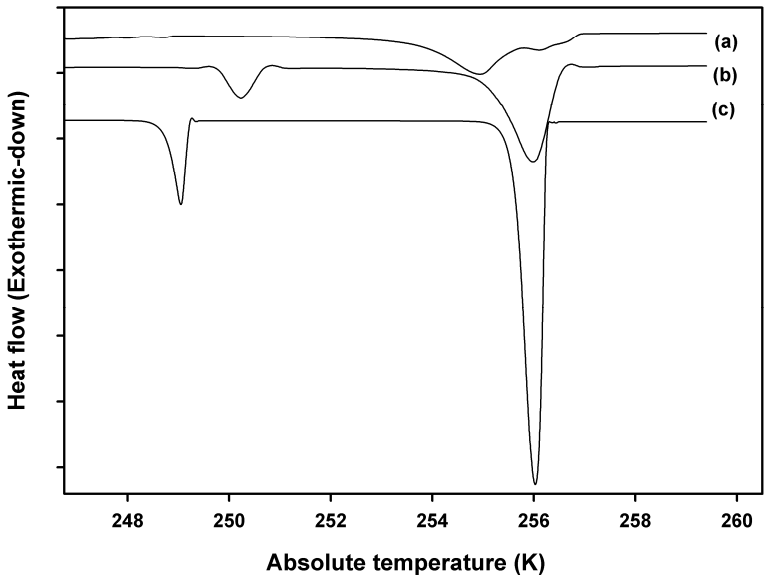

Figure 7 DSC freezing traces of water in the samples of CCS equilibrated with (a) 96% RH, (b) 100%RH, and (c) liquid water. It is noted that hydrogels of other polymer under study also exhibit similar behavior.

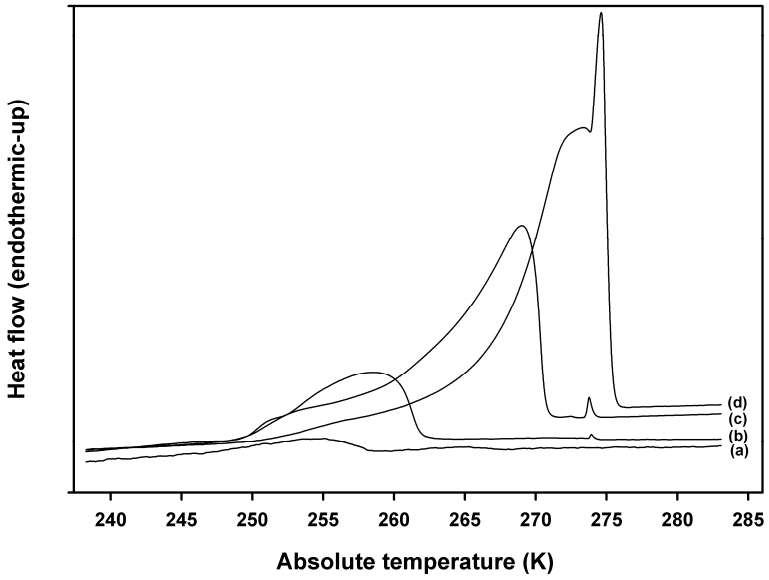

Figure 8 DSC endothermic melting of ice in SSG equilibrated with (a) 84% RH, (b) 96% RH, (c) 100% RH, and (d) excess liquid water (fully hydrated). It is noted that hydrogels of other polymer under study also exhibit similar behavior.

Non-freezable bound water

An attempt in the determination of water of fraction (i) for each of polymer-water systems was made and tabulated in Table 2. The materials under study exhibit the non-freezable water contents of between 9.67% and 26.63% whereas it was previously reported that starches and celluloses exhibited non-freezable bound water contents of 28% (Zhong & Sun, 2005) and 22-25% (Luukkonen at al., 2001), respectively. McCrystal et al (1997) estimated the number of moles of non-freezing water per polymer repeating unit HPMC gel as approximately 3.8 moles that is corresponding to approximately 10-20% water content dependent on degrees of substitution, while the current study on HPMC is within the range (13.21%, Table 2). On the other hand, the cross-linked chemically modified starch and cellulose that are more hygroscopic (SSG and

CCS) illustrate low level of non-freezable bound water (Table 2). It might be because these materials present more number of ice nuclei, during freezing, that draw more water molecules due to hydrogen bonding to the ice clusters as a process of lowering surface free energy. As a result more portion of freezable water may be detected.

Polymeric material	[1]Overall water content (%)	[2]Freezable water content (%) (mean, s.d.)	[3]Water of fraction (i) (%)	[4] φ_{2V}
PS	80.01	53.38, 1.09	26.63	0.112
SA	73.36	47.43, 1.07	25.93	[a]0.167
SSG	73.28	52.30, 1.11	20.98	0.031
HPMC	51.30	38.09, 0.87	13.21	[a]0.384
SCMC	69.13	46.14, 0.78	22.99	0.145
CCS	79.97	70.30, 1.11	9.67	0.054

1. Overall water content was determined by moisture balance.
2. Freezable water content was determined by DSC traces calculation (in 3 replicates) based on the heat of melting in Table 1.
3. Non-freezable water content was calculated as Overall water content minus Freezable water content.
4. The fully hydrated polymer volume fraction based on equation (Mantovani et al., 2000): $\phi_{2V} = \left[\overline{d_{al}}/\overline{d_w}\right]^3$ where $\overline{d_{al}}$ and $\overline{d_w}$ are geometric mean volume diameters of a powdered polymer in alcohol and in water, respectively.

a. The numbers are taken from reference (Mutalik et al., 2006) since the equipment could not determine.

Table 2 Water contents and the volume fractions of fully hydrated hydrophilic polymers under study

The thermodynamic relation for a polymer solution

A general thermodynamic theory of polymer solution based on mixing according to liquid lattice theory has been presented by Flory (1971). For polymeric hydrogels employed in the present study, the chemical potential of water in a water-polymer system includes not only Flory's mixing with swollen gel but the Donnan equilibrium for polyelectrolytes that yields the following relationship (Flory, 1971, Okoroafor et al. 1998, Mantovani et al. 2000, Ozmen & Okay, 2005, and Borchard et al. 2005):

$$(1) \qquad \mu_1^{gel} - \mu_1^0 = RT[\ln(1-\varphi_2) + \varphi_2 + \chi_1\varphi_2^2 + V_1(\frac{v_e}{V_0})(\varphi_2^{1/3} - \frac{\varphi_2}{2}) - f \cdot \varphi_2]$$

Where, φ_2, χ_1, v_e , and f are volume fraction of polymer in gel, the polymer-water interaction parameter, the effective crosslink density of the network, and the fraction of charged units in the hydrogel network, respectively. V_1 and V_0 are molar volume of water and the volume of relaxed hydrogel network. R and T are gas constant and absolute temperature. μ_1^0 is the chemical potential of pure liquid water. And, μ_1^{gel} is the chemical potential of water in hydrogel. The first three terms in the right hand side of equation 1 represent the chemical potential of general polymer-water mixture. The fourth term is the chemical potential due to reaction of the network crosslink structure (Flory, 1971), whereas the last term is that from Donnan equilibrium theory (Mantovani et al. 2000, and Ozmen & Okay, 2005).

It is further assumed that frozen water is in equilibrium with the unfrozen water in gel phase during the DSC operation, i.e., the chemical potential of freezing ice (μ_1^{ice}) and of water in hydrogel (μ_1^{gel}) must be equal. And when a mixture freezes, one of the colligative properties known as freezing point depression holds. The change of chemical potential can be written as (Ozmen & Okay, 2005):

(2) $$\mu_1^{ice} - \mu_1^0 = \Delta H_m(\frac{T}{T_0} - 1)$$

Where ΔH_m, and T_0 are molar enthalpy of crystallization (or melting), and melting temperature of pure water, respectively. Since the left hand side of equation 1 and 2 are equal, the arrangement of these two equations yields:

(3) $$\frac{1}{T} = \frac{1}{T_0} - \frac{R}{\Delta H_m} \cdot [\ln(1-\varphi_2) + \varphi_2 + \chi_1 \varphi_2^2 + V_1(\frac{v_e}{V_0})(\varphi_2^{1/3} - \frac{\varphi_2}{2}) - f \cdot \varphi_2]$$

This equation should be applicable to the water of fraction (ii) where the ice-liquid water transition temperature was depressed. And, assuming the involved parameters are constant over the transition temperature, the parameters such as χ_1 could be obtained by non-linear regression of $\frac{1}{T}$ as a function of φ_2 according to the model described by equation 3.

The volume fraction of polymeric hydrogels vs. melting depression: non-linear fitting to the Flory's model

The volume fractions in liquid water ($\varphi_{2\,V}$'s) of fully hydrated polymers under study are tabulated in Table 2. It is noted that $\varphi_{2\,V}$'s of SA and HPMC have

been taken from the reference (Mutalik et al., 2006) since the polymers dissolved in water and alcohol, respectively. φ_{2V}'s of sodium starch glycolates have been previously reported as the numbers between 0.005 and 0.045 (Mantovani et al., 2000) whereas $\varphi_{2\,V}$ of SSG which is chemically identical is 0.031 (Table 2). In addition, the DSC melting traces yield the endotherms closed to 0 °C compared to the exotherms of freezing traces (Figures 3 and 8). Thus the endothermic melting transition of a fully hydrated polymer is used in order to have an appropriate φ_2.

Polymeric material	χ_1 Estimate, SE	$V_1\frac{v_e}{V_0}$ Estimate, SE	f Estimate, SE	r^2
PS	0.761, 0.041	0.067, 0.017	**-	0.9399
SA	0.738, 0.033	*-	0.513, 0.022	0.9864
SSG	0.520, 0.051	0.084, 0.010	0.288, 0.093	0.9941
HPMC	0.847, 0.032	*-	**-	0.9339
SCMC	0.776, 0.021	*-	0.368, 0.070	0.9467
CCS	0.679, 0.025	[a] 0.028, 0.048	0.241, 0.002	0.9999

* Since the polymers are linear, network contribution is absent.
**Since the polymers are uncharged, the reduced model with $f = 0$ is used.
[a] The contribution is statistically non-significant at 0.05 α-level.

Table 3 The estimates of the parameters according to the restricted ($R/\Delta H_m$ = 1.383 x 10^{-3} K^{-1} and T_0 = 273.15 K) non-linear regression of equation 3.

Each of φ_2-T data sets derived from DSC curves was non-linearly fitted into equation 3 with the restricted conditions that ($R/\Delta H_m$) = 1.383 x 10^{-3} K^{-1} (Borchard et al., 2005). The estimates as well as their standard errors (SE) of parameters including χ_1, network factor ($V_1\frac{v_e}{V_0}$) and f are tabulated in Table 3. It is noted that ionic and/or cross-linking network contribution factor was set as null for uncharged and/or linear polymers, respectively. It was found that the model is

successfully applied to φ_2-T data sets with high correlations (r^2 between 0.9339-0.9941: Table 3). It is thus demonstrated that χ_1, charges, and polymer network affect the crystallization / melting of water that the polymer contains.

As see in Table 3, f's of charged polymers are statistically significant from null at α-level of 0.05, so are network factors of cross-linked ones except CCS. f reflects the degree of ionization whereas network factor illustrates swelling of the cross-linked polymers (Borchard et al., 2005, and Mantovani et al., 2000). It is observed that at 0.05-α-level, network factor in the case of CCS is not significantly different from null. It might evidently be because the swelling of the polymeric network is not sufficient to significantly effect on the water crystallization / melting for it was previously reported that the swelling capacity of CCS present in water was far lower than that of SSG (Visavarungroj & Remon, 1990). In addition, Okoroafor, et al. (1998) mentioned that the effect of network factor was quite small since its value usually is of the order of two decimal digits. That is consistent with the current study as it is observed that the estimates of network factor are in the same order of magnitude (Table 3).

Flory's interaction parameter (χ_1)

To characterize the thermodynamic interaction between water and polymer, Flory (1971) introduced a dimensionless quantity: χ_1. It represents merely the difference in energy divided by thermal agitation energy (kT: where k is Boltzmen's constant) of a solvent molecule immersed in the pure polymer compared with one surrounded by molecules of its own kind. A number of authors

reported the magnitudes of χ_1 of aqueous polymeric solutions including starches and its derivatives (Baks et al., 2007; Cruz-Orea et al., 2002; Mantovani et al., 2000; Farhat & Blanshard, 1997), and sodium alginate (Borchard et al., 2005) as the numbers ranging between 0.43 and 0.67. As seen in Table 3, the estimates of χ_1-parameters of the same types of polymers vary between 0.520 and 0.761 which are slightly higher. In fact, the magnitude χ_1 is not a constant. It is dependent on volume fraction as well as temperature (Myagkova et al., 1997 and Flory, 1971). Thus experimental conditions should play an important rule on its magnitude especially during the initial setting causing the deviation of χ_1 values from laboratories to laboratories. Myagkova et al. (1997) mentioned that the χ_1 should be approximately 0.5 for maximum dissolving capacity of liquid water, i.e., the good-solvent conditions, for cellulose esters whereas the magnitudes of χ_1 for the same type of polymers under study are 0.679-0.847 which also approaches those conditions.

Figure 9 illustrates the plot of χ_1 versus the reciprocal absolute temperature of the onset of DSC melting transition of water of fraction (ii) in fully hydrated samples. It is found that the smaller the value of χ_1, the larger solvent water melting was depressed, i.e., stronger affinity for water. Flory (1971) rectified the energy quantity of χ_1 that should be regarded as the free energy change rather than as the heat of mixing only. χ_1 then contains an entropy contribution in addition to enthalpy one. Thus, in a simple case (Borchard et al., 2005):

(4) $$\chi_1 = \alpha_1 + \frac{\beta_1}{T}$$

where, α_1 and β_1 are entropy and enthalpy parameters, respectively. As seen in Figure 6, the trend line as well as 95% confidence interval (dotted lines in Figure 5) represents the data fitting according to equation 4. Unfortunately, the power of regression and the correlation coefficient are as low as 25.01% and 0.631, respectively. It might be because the nature of individual polymers and experimental conditions could complicate the systems resulting the fitted parameters are so empirical that they are meaningless to address.

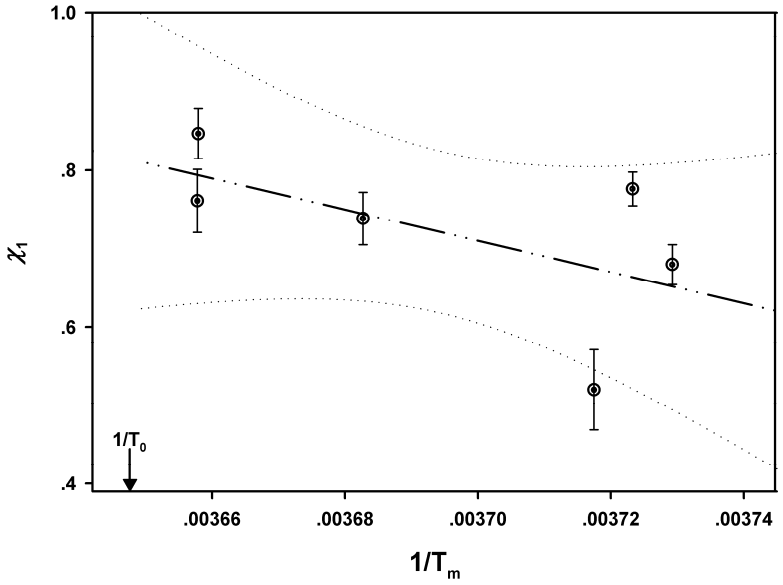

Figure 9 The plot of χ_1-parameter against the reciprocal of onset temperature (in absolute scale) of melting transition of freezable bound water in water-polymer systems under study.

Freezable bound water vs. thermoporometry

In hydro-polymeric gel, liquid water may occupy the space within structural network formed by swollen polymers and should be called hydro-pores.

The freezable bound water characterized at a temperature few degrees below 273.15 K has been interpreted either as due to the interaction between water and polymer functional groups (Zografi and Kontny, 1986) or capillary condensation within hydro-pores (Hay and Laity, 2000). The former, on one hand, may associate with polymer swelling and dissolution since hydrophilic polymer for example SA may partially dissolve in water (Huang et al, 1999.) i.e., the system behaves as a polymer solution. On the other hand, a number of authors (Ishikiriyama and Todoki, 1995; Hay and Laity, 2000; Faroongsarng and Peck, 2003; Yamamoto et al, 2005) examined the pore sizes and distributions of various materials assuming that water is mostly held within pores, with melting temperature being depressed by Gibbs-Thomson effect. The relationship between radius (r_k) and temperature depression (ΔT) is described by equation 5.

$$r_k = \frac{2\gamma V_l \cdot T_m}{\Delta H_0 \cdot \Delta T} \quad (5)$$

Where, ΔH_0, γ, V_l, and T_m are molar heat of melting, surface tension of liquid water (1.72×10^{-6} cal/cm^2), molar volume of water (18 cm^3/mol), and melting temperature, respectively. The radius in equation 1 is not exactly the radius of the porosity since there are non-freezable water layers attached pore surface. The pore radius could be calculated according to empirical equation (. Ishikiriyama and Todoki, 1995; Yamamoto et al, 2005a, Landry, 2005; Yamamoto et al, 2005b):

$$r = \frac{\alpha(T)}{\Delta T} + \beta \quad (6)$$

Where, the first term is equivalent to equation 5, the second term is the correction due to non-freezable bound water. The hydro-pore sizes and distributions may be determined via the water endotherms using equation 5 whereas β-correction should be excluded as a part of the swollen polymer network.

Previous reports always considered only one phenomenon by assuming the other was negligible dependent upon the nature of systems under study (Ishikiriyama and Todoki, 1995; Hay and Laity, 2000; Ping et al, 2001; Faroongsarng and Peck, 2003; Yamamoto et al, 2005). In fact, both polymer-water interaction and condensation within hydro-pores may spontaneously and continuously occur. It is thus assumed that there are 3 clusters of freezable water including: 1) bound water with specific sites on polymer, 2) water condensation within swollen polymer network (hydro-pore water), and 3) water-polymer gelation associated with bulk water (polymer solution). As seen in Figure 8, the frozen water tracing of bound fraction moved close to that of bulk one with increasing amount of water, and combine each other where water in excess present, i.e., free water crystallizes as the expense of bound water crystalline. With water in excess, the clusters of water dynamically transfer from hydro-pore water to gelation as the swollen polymers are unfastening their network structure in order to decrease surface free energy resulting in hydrogel formation. As a result the evidence of hydro-pores could not be detected as some authors concluded that the melting depression is due not to water confinement in polymer network but rather to water-polymer interaction (Rault et al, 1994; Okoroafor et al, 1998). Thus, to examine the hydro-pore structure if present, the system should

contain only a limit amount of water which being frozen to prevent the movement of hydro-pore water to hydrogel.

It has been suggested that the DSC tracing of a hydrophilic polymer pre-treated with 96-100%RH should be used in thermoporometry (Faroongsarng and Peck, 2003), i.e., the amount of water in a polymer is limited by the aqueous affinity of its own where water content is just insufficient to hydrogel formation. Furthermore, the freezable bound water might consist of more than one endothermic peak for asymmetry was observed. The endotherm then might be interpreted as 2 phenomena including bound water cluster and hydro-pore condensation. With the aid of in-house software for shape analysis, the endothermic peaks of freezable bound water of 100%RH pre-treated SA and SSG were sub-divided into 2 parts and showed in Figures 10-11.

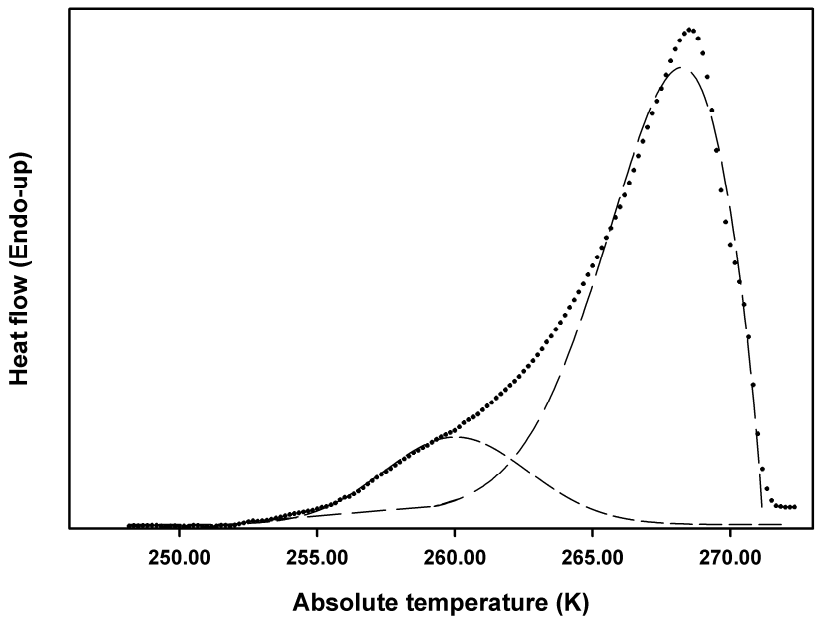

Figure 10 The endothermic peak separation of an endotherm corresponded to freezable bound water of SA. The peak temperatures of hydro-pore water, and water for swelling/dissolution is 263.51, 260.02 K, respectively.

It is proposed that the majority of endotherm may be the water in hydro-pores whereas the minor one may be water associated with polymer swelling and dissolution. On one hand, equation 1 was utilized for transformation of the abscissa of the DSC curves of each of the sub-divided endothermic peaks in Figures 10 and 11 (those with peak temperatures of 263.51 and 269.02 K) to the hydro-pore radii. On the other hand, the corresponding size distributions of water within hydro-pores ($\frac{dV}{d\,r_k}$) can be obtained by equation 3 (Yamamoto at al, 2005a; Yamamoto at al, 2005b; Landry, 2005):

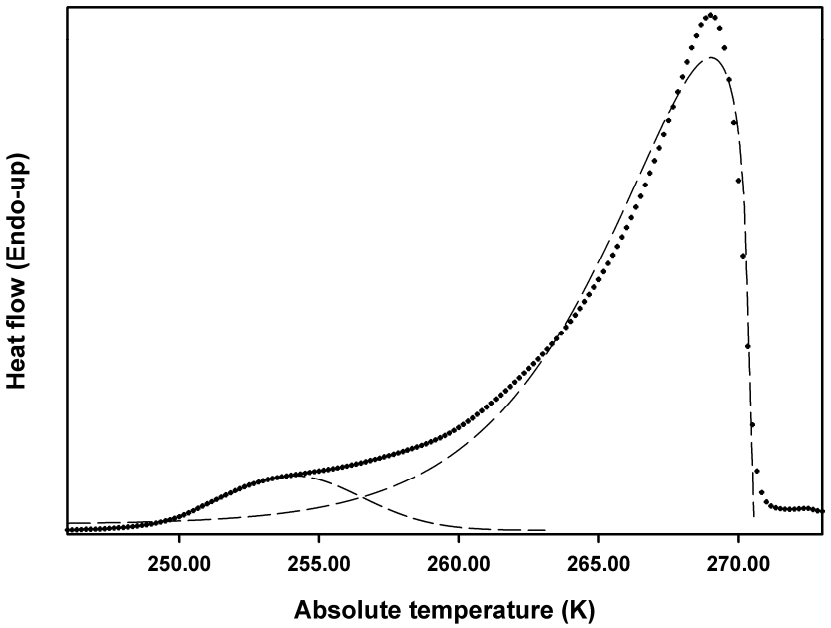

Figure 11 The endothermic peak separation of endotherm corresponded to freezable bound water of SSG. The sub-endothermic peaks were based on non-linear fitting of Gaussian, logarithmic normal, or Weibull distribution model according to best fit. The peak temperatures of hydro-pore water, and water for swelling/dissolution is 269.02, 254.04 K, respectively.

$$\frac{dV}{d\,r_k} = \frac{dq}{dt}\frac{dt}{dT}\frac{dT}{d\,r_k}\frac{1}{\rho(T)\cdot\Delta H(T)_m} \qquad (7)$$

Where, V, dq/dt, and dt/dT are volume of water, heat flow, and the reciprocal of heating rate, respectively. $\rho(T)$ and $\Delta H(T)_{\mathrm{m}}$ are density and enthalpy changes of freezable hydro-pore water. They are dependent upon absolute temperature as described by the empirical equations previously proposed (Landry 2005; Yamamoto et al, 2005a; Yamamoto et al, 2005b):

(8) $$\rho(T) = -7.1114 + .0882T - 3.1959 \times 10^{-4} T^2$$

(9) $$\Delta H(T)_{.m} = 334.1 + 2.119(T - T_m^0) - .00783\,(T - T_m^0)^2$$

Where, T_m^0 is the equilibrium melting temperature of water. The hydro-pore distributions of both SA and SSG hydrogels were plotted against hydro-pore radii in Figure 12.

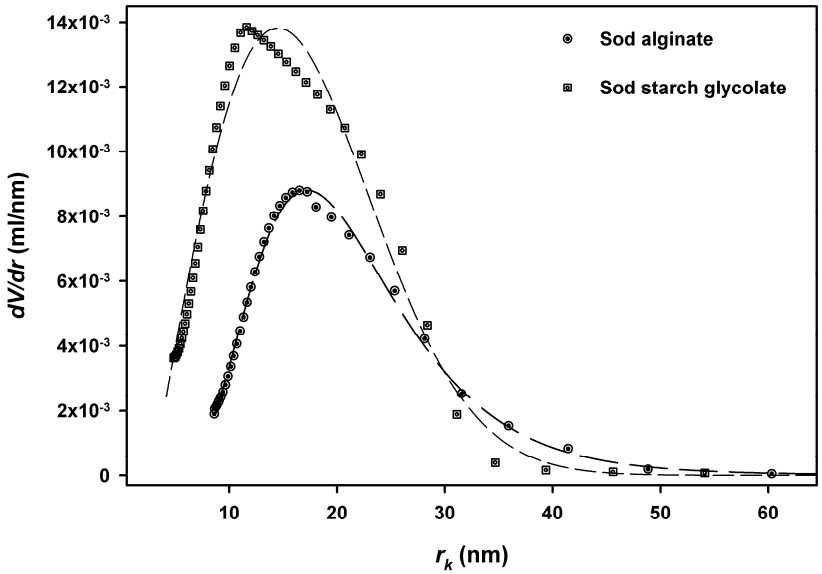

Figure 12 Hydro-pore distributions of polymeric gels under study

It was observed from Figure 12 that SSG hydrogel exhibit the hydro-pore volume grater than that of SA one whereas the hydro-pore radii were comparable. The distributions were fitted into a logarithmic normal distribution model in order

to determine average pore radii. The pore distribution data were very well fitted with r^2 of 0.9964 (SA gel) and 0.9358 (SSG gel). It was found that the geometric means (standard deviations) of hydro-pore radii in SA and SSG gels are 17.19 (1.48) and 13.03 (1.72) nm, respectively.

Thermoporosity compared with Adsorption BHJ pore size distribution

The carbohydrate polymers including SA and SSG in dry state were subjected to the pore size determination by mean of nitrogen adsorption technique. The BHJ pore size distributions, ranging between 6 and 160 nm, of surfaces of SA and SSG are showed in Figures 13 and 14. It is noted that this pore size range is classified as mesopores and is commonly obtained by nitrogen adsorption technique. Not only mesopores, but the surfaces of SA and SSG also showed macropores in a few micrometers in size as seen in electron micrographs (Figure xxx of the previous section). In term of macropores, SSG presented somewhat smooth surface, but SA exhibited a few micrometer-sized porosity.

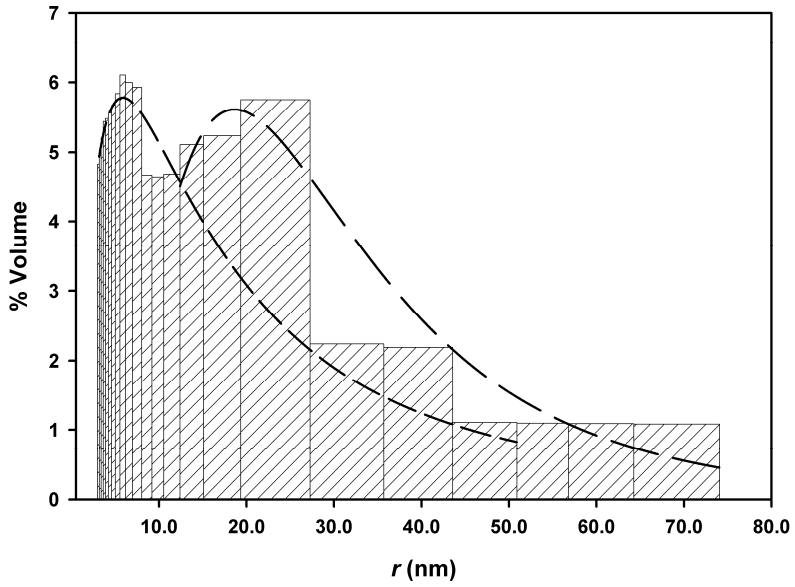

Figure 13 Nitrogen adsorption BHJ pore size distribution on the surface of dry powders of SA. The broken lines illustrate the curve fitting according to logarithmic-normal distribution.

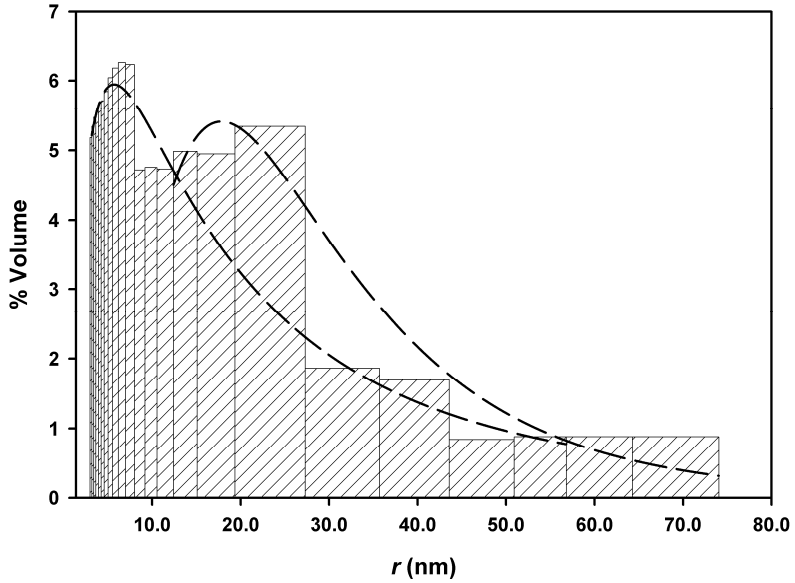

Figure 14 Nitrogen adsorption BHJ pore size distribution on the surface of dry powders of SSG. The broken lines illustrate the curve fitting according to logarithmic-normal distribution.

As seen in Figures 13-14, the mesopore distribution on SA and SSG surface could sub-divided into 2 groups as both exhibit a bi-modal distribution.

The logarithmic-normal distribution model is utilized to determine the means and standard deviations of sub-grouped pore radii and tabulated in Table 4.

Material	Geometric mean: nm (SE of estimate)	Geometric S.D.: nm (SE of estimate)	R^2 of fitting
SA			
Smaller radius	5.86 (0.51)	0.55 (0.08)	0.943
Larger radius	18.63 (3.03)	0.31 (0.08)	0.890
SSG			
Smaller radius	5.70 (0.57)	0.57 (0.06)	0.971
Larger radius	17.83 (3.11)	0.30 (0.08)	0.897

Table 4 The sub-grouped radii of BHJ pore size distributions on the surfaces of dry powders of SA and SSG determined by nitrogen adsorption.

However the macropores on SA and SSG were totally different, it is observed that the mesopore distributions of these two polymeric surfaces are practically identical (Table 4 and Figures 13-14). The mean radii of larger size pore groups of dry surfaces of SA and SSG were 18.63 nm and 17.83 nm, respectively. Although they are slightly greater, the pore sizes may be comparable to those of hydro-pores (17.19 and 13.03 nm for SA and SSG, respectively). It is thus suggested that the thermoporometric determination by this technique might be valid for some portion of porosity on the surface of hydrophilic polymers. And, the geometric standard deviations of hydro-pores were narrower compared with those of BHJ. It might be because the treatment excluded few water layers with swollen polymer network (β-parameter in equation 2) that the size distribution could be restricted. Unfortunately, the smaller size range of the porosity showed in BHJ pore distribution could not be seen by thermoporometry. A minority portion of a DSC endotherm was previously discarded since it was proposed as the water associated with polymer swelling and dissolution whereas there may include pore

confinement. In addition, the size range of around 5-6 nm reported by nitrogen adsorption might not be determined by thermoporometry since it is equivalent to the swollen polymer thickness where the associate water might not be frozen.

In summary, carbohydrate polymers including SA and SSG could form structural hydro-pores within polymeric gel having the average radii of approximately 20 nm. In hydrogel drug delivery, the drug molecules must travel via these hydro-pores. Thus, the hydro-pore size and distribution may play a significant role in hydrogel drug release. It is further suggested that the drug with a molecular size of approximately 30-50 nm may controllably diffuse through these hydrogels since the size is comparable with that of hydro-pores of the gels.

References

Adamson, AW. 1990. Physical chemistry of surface, 5th ed., A Wiley-Interscience Publication, New York.

Baks, T, Ngene, I S, van Soest, J J G, Janssen, A E M and Boom, R M. 2007. Comparison of methods to determine the degree of gelatinisation for both high and low starch concentrations. *Carbohyd Polym*. 67: 481-490.

Borchard, W, Kenning, A, Kapp, A, and Mayer, C. 2005. Phase diagram of the system sodium alginate/water: A model for biofilms. *Int J Biol Macromole*. 35: 247-256.

Dean, JA. 1985. Lange's Handbook of chemistry, 13rd Ed., McGraw-Hill, New York, p. 9-117.

Edge, S. et al. 2002. Chemical characterization of sodium starch glycolate particles. *Int J Pharm*. 240: 67-78.

Faroongsarng, D. and Peck, GE. 2003. Thermal porosity analysis of croscarmellose sodium and sodium Starch Glycolate by differential scanning calorimetry. *AAPSPharmSciTech*. 4(4): article 67.

Flory, P J. 1971. *Principles of polymer chemistry*. Cornell University Press, Ithaca and London.

Hay, JN. and Laity, PR. 2000. Observation of water migration during thermoporometry studies of cellulose films. *Polymer*. 41: 6171-6180.

Higuchi, A and Iijima, T. 1985. DSC investigation of the states of the water in poly(vinyl alcohol) membranes. *Polymer*. 26: 1207-1211

Huang, RYM., Pal, R., and Moon, GY. 1999. Characteristics of sodium alginate membranes for the prevaporation dehydration of ethanol-water and isopropanol-water mixture. *J Memb Sci*. 160: 101-113.

Ishikiriyama, K, and Todoki, M. 1995. Pore size distribution measurements of silica gels by means of differential scanning calorimetry. *J Colloid Interf Sci*. 171: 103-111.

Landry, MR. 2005. Thermoporometry by differential scanning calorimetry: experimental considerations and applications. *Thermoc acta*. 433: 27-50.

Lavine, H, and Slade, L. 1988. Water as a plasticizer: Physico-chemical aspects of low-moisture polymeric systems. In: Franks, F. Ed. Water surface review, Cambridge University Press, New York, p. 75-185.

Luukkonen, P, Maloney, T, Rantanen, J, Paulapuro, H, and Yliruusi J. 2001. Microcrystalline cellulose-water interaction-A novel approach using thermoporosimetry. *Pharm Res*. 18(11): 1562-1569.

Mantovani, F, Grassi, M, Colombo, I, and Lapasin, R. 2000. A combination of vapor sorption and dynamic laser light scattering methods for the determination of the parameter χ and the crosslimk density of a powdered polymeric gel. *Fluid Phase Equilibr*. 167: 63-81.

McCrystal, CB, Ford, JL and Rajabi-Siahboomi A R. 1997. A study on the interaction of water and cellulose ethers using differential scanning calorimetry. *Thermochim Acta*. 294: 91-98.

Mutalik, V, Manjeshwar, LS, Wali, A, Sairam, M, Raju, KVSN and Aminabhavi T M. 2006. Thermodynamics/hydrodymanics of aqueous polymer solutions and dynamic mechanical characterization of solid films of chitosan, sodium alginate, guar gum, hydroxyl ethyl cellulose and hydroxypropyl methylcellulose at different temperatures. *Carbohyd Polym*. 65: 9-21.

Myagkova, NV, Rakhmonberdiev, GR, Sagdieva, ZG and Sidikov AS. 1997. Thermodynamic properties of solutions of water-soluble mixed cellulose esters. *Chem Nat Compd*. 33(1): 76-79.

Nakamura, K, Hatakeyama, T and Hatakeyama, H. 1981. Studies on bound water of cellulose by differential scanning calorimetry. *Tex Res J*. 51(9): 607-613.

Okoroafor, EU, Newborough, M, Highgate, D and Augood, P. 1998. The thermal behaviour of water in crosslinked hydro-active polymeric structure: crystasllization of water. *J Phys. D: Appl Phys*. 31: 3120-3129.

Ozmen, MM and Okay, O. 2005. Superfast responsive ionic hydrogels with controllable pore size *Polymer*. 46: 8119-8127.

Ping, ZH. et al. 2001. States of water in different hydrophilic polymers-DSC and FTIR studies. *Polymer*. 42: 8461-8467.

Rajabi-Siahboomi, AR, Bowtell, RW, Mansfield P, Davies MC & Melia C D. 1996. Structure and Behavior in Hydrophilic Matrix Sustained Release Dosage Forms: 4. Studies of Water Mobility and Diffusion Coefficients in the Gel Layer of HPMC Tablets Using NMR Imaging. *Pharm Res*. 13(3): 376-380

Rault, J, Gref, R, Ping, ZH, Nguyen, QT and Neel, J. 1995. *Polymer*. 36: 1655-31.

Sair, L, and Fetzer, WR. 1944. *Ind. Eng. Chem*. 36: 205.

Visavarungroj, N and Remon, JP. 1990. Crosslinked starch as a disintegrating agent. *Int J Pharm*. 62: 125-131.

Yamamoto, T. at al. 2005a. Evaluation of porous structure of resorcinol-formaldehyde hydrogels by thermoporometry. *Thermochim acta*. 439: 74-79.

Yamamoto, T. et al. 2005b. Evaluation of thermoporometry for characterization of mesoporous materials. *J Colloid Interface Sci*. 284: 614-620.

Zhong, Z and Sun, XS. 2005. Thermal characterization and phase behavior of cornstarch studied by differential scanning calorimetry. *J Food Eng*. 69: 453-459.

Zografi, G, Kontny, MJ. 1986. The interactions of water with cellulose- and starch-derived pharmaceutical excipients. *Pharm Res*. 3(4): 187-194.

Output ที่ได้จากโครงการ

Faroongsarng, D., and Sukonrat, P. Thermal behavior of water in polymeric hydrogels of the selected pharmaceutical excipients. *Int. J. Pharm*. Submitted and under review.

Elsevier Editorial System(tm) for International Journal of Pharmaceutics

Manuscript Draft

Manuscript Number: IJP-D-07-00617

Title: Thermal behavior of water in polymeric hydrogels of the selected pharmaceutical excipients

Article Type: Research Paper

Section/Category:

Keywords: freezable water, water-polymer interaction, Flory's interaction parameter (χ1), melting point depression, hydrogel

Corresponding Author: Associate Professor Damrongsak - Faroongsarng, Ph.D.

Corresponding Author's Institution: Prince of Songkla University

First Author: Damrongsak - Faroongsarng, Ph.D.

Order of Authors: Damrongsak - Faroongsarng, Ph.D.; Patchara - Sukonrat

Abstract: In a polymer-water matrix, freezable water is depressed due to either porosity confinement or interaction. The aim of the study was to examine water crystallization/melting depression by sub-ambient differential scanning calorimetry. The selected starch and cellulose based excipients including pre-gelatinized starch (PS), sodium alginate, sodium starch glycolate, hydroxypropylmethyl cellulose (HPMC), sodium carboxymethyl cellulose, and croscarmellose sodium were employed. The pre-treated with ambient humidity (85-100% relative humidity, at 30.0±0.2°C for 10 days) and with excess water (hydrogels) samples were subjected to a 25 - -150°C-cooling-heating cycle at 5.00 °C/min rate. The volume fractions of hydrogels were measured by light scattering technique. It was observed that all polymers but PS and HPMC with ambient humidity presented freezable water in two distinct fractions namely bound water where crystallizing/melting temperature was depressed and bulk water. The water transition in samples with various contents exhibited the pattern as a polymer solution, thus rather than confinement, the depression was due to interaction. The volume fraction-melting temperature data derived from endotherms of hydrogels were successfully fitted to Flory's model (r2: 0.934-0.999). The Flory's interaction parameters (χ1) were found to vary between 0.520 and 0.847. In addition, the smaller the value of χ1, the larger melting was depressed, i.e., stronger affinity for water.

were successfully fitted to Flory's model (r2: 0.934-0.999). The Flory's interaction parameters ($\chi 1$) were found to vary between 0.520 and 0.847. In addition, the smaller the value of $\chi 1$, the larger melting was depressed, i.e., stronger affinity for water.

*** Letter of Submission**

Faculty of Pharmaceutical Sciences
Department of Pharmaceutical Technology
Prince of Songkla University, Hat Yai, Thailand 90112.

June 13, 2007

Dear Editor:

I would like to submit the manuscript entitled: "Thermal behavior of water in polymeric hydrogels of the selected pharmaceutical excipients" to *Int. J. Pharm*. The manuscript describes the crystallization/melting depression of water present in hydrogels of various polymeric pharmaceutical excipients used in drug delivery dosage forms that could be detected by differential scanning calorimetry. We derived the information from DSC tracings and the obtained information was successfully modeled using Flory's polymer solution theory.

Although the DSC technique is not new, the manuscript could provide the novel insight into the thermodynamic principles of polymer-water interaction.

Sincerely,

Damrongsak Faroongsarng, Ph.D.

IJP AUTHOR CHECKLIST

Dear Author,

It frequently happens that on receipt of an article for publication, we find that certain elements of the manuscript, or related information, is missing. This is regrettable of course since it means there will be a delay in processing the article while we obtain the missing details.

In order to avoid such delays in the publication of your article, if accepted, could you please run through the list of items below and make sure you have completed the items.

Overall Manuscript Details

- Is this the final revised version? ☑
- Are all text pages present? ☑
- Are the corresponding author's postal address, telephone and fax numbers complete on the manuscript? ☑
- **Have you provided the corresponding author's e-mail address?** ☑
- **Manuscript type – please check one of the following:**
  - Full-length article ☑
  - Review article ☐
  - Rapid Communication ☐
  - Note ☐
  - Letter to the Editor ☐
  - Other ☐
- **Manuscript section – paper to be published in:**
  - Pharmaceutical nanotechnology section ☐

Manuscript elements

- Short summary/abstract enclosed? ☑
- 3-6 Keywords enclosed? ☑
- Complete reference list enclosed? ☑
- Is the reference list in the correct journal style? ☑
- Are all references cited in the text present in the reference list? ☑
- Are all **original** figures cited in the text enclosed? ☑
  Electronic artwork format? ----------
- Are figure legends supplied? ☑
- Are all figures numbered and orientation provided? ☑
- Are any figures to be printed in colour? ☐
  If yes, please list which figures here:----------
- If applicable, are you prepared to pay for reproduction in colour? ☐
- Are all tables cited in the text supplied? ☑

General

- Can you accept pdf proofs sent via e-mail? ☑

*** Manuscript**

Title: Thermal behavior of water in polymeric hydrogels of the selected pharmaceutical excipients

Authors and affiliations:

*Damrongsak Faroongsarng
Drug Delivery Systems Research Center, Department of Pharmaceutical Technology, Faculty of Pharmaceutical Sciences, Prince of Songkla University, Hat Yai 90112, Thailand.

Patchara Sukonrat
Scientific Equipment Center, Prince of Songkla University, Hat Yai, 90112, Thailand.

*Corresponding author
e-mail: damrongsak.f@psu.ac.th
Phone: +66-74-288-841
FAX: +66-74-428-148

Thermal behavior of water in polymeric hydrogels of the selected pharmaceutical excipients

Abstract

In a polymer-water matrix, freezable water is depressed due to either porosity confinement or interaction. The aim of the study was to examine water crystallization/melting depression by sub-ambient differential scanning calorimetry. The selected starch and cellulose based excipients including pre-gelatinized starch (PS), sodium alginate, sodium starch glycolate, hydroxypropylmethyl cellulose (HPMC), sodium carboxymethyl cellulose, and croscarmellose sodium were employed. The pre-treated with ambient humidity (85-100% relative humidity, at 30.0±0.2°C for 10 days) and with excess water (hydrogels) samples were subjected to a 25 - -150°C-cooling-heating cycle at 5.00 °C/min rate. The volume fractions of hydrogels were measured by light scattering technique. It was observed that all polymers but PS and HPMC with ambient humidity presented freezable water in two distinct fractions namely bound water where crystallizing/melting temperature was depressed and bulk water. The water transition in samples with various contents exhibited the pattern as a polymer solution, thus rather than confinement, the depression was due to interaction. The volume fraction-melting temperature data derived from endotherms of hydrogels were successfully fitted to Flory's model (r^2: 0.934-0.999). The Flory's interaction parameters (χ_1) were found to vary between 0.520 and 0.847. In addition, the smaller the value of χ_1, the larger melting was depressed, i.e., stronger affinity for water.

Keywords: freezable water, water-polymer interaction, Flory's interaction parameter (χ_1), melting point depression, hydrogel.

1. Introduction

Starch and cellulose based materials derived from naturally occur biopolymers are the major pharmaceutical excipients utilized in drug delivery dosage forms. These polymers always interact with water due to their hydrophilicity exhibiting some properties that may critically affect the dosage form performance. For example: In controlled release devices, water diffusion through a polymeric hydrogel layer has been considered as one of the major factors determining drug release rate (Rajabi-Siahboomi, et al., 1996). With liquid water in excess, these hydrophilic polymers could form hydrogels i.e., the three-dimensional arrangement possessing the ability to retain a significant fraction of water without complete dissolving. A hydrogel might form relatively stable space lattice or network pores fulfilled with a considerable amount of water. The interfacial tension related to surface of curvature of water within pores could develop and affect the phase transition of the water. Thus this phase transition of water confinement could somehow characterize the pores where it occupies. A number of authors, for examples: Yamamoto at al. (2005), Faroongsarng & Peck (2003), Hay & Laity (2000), and Ishikiriyama & Todoki (1995) examined the pore sizes and distributions of various porous materials assuming that water is mostly held within pores, with melting temperature being depressed by Gibbs-Thomson effect. However, the depression of melting temperature is not only attributed by water confinement in porosity but the water-polymer interaction. Rault et al (1994) reported that the melting depression and the concentration of unfrozen water varied with the water concentration with similar orders of magnitude for polymer-water systems and simple binary mixtures, presenting the same type of interaction, from which confinement effects are absent. They concluded that the melting depression is due not to water confinement in polymer network porosity but rather to water-polymer interactions. The evidence was later confirmed by the work of Okoroafor et al (1998).

In general, interactions between macromolecules fall into four categories: ionic, hydrophobic, van der Waals and hydrogen bonding (Ilmain, et al., 1991). But for a polymer-water mixture, the interaction is always in the range of hydrogen bonding. It has been proposed (Ping, et al., 2001; Zografi & Kontny, 1986; and Higuchi & Iijima, 1985) that water in hydrophilic polymer matrices presents in three distinct fractions: (i) non-freezable bound water, (ii) freezable bound water, and (iii) free or bulk water. Upon cooling, water begins to crystallize only when its content is above a characteristic threshold. This fraction of water has been called freezable bound water (fraction (ii)) because it exhibits a melting point lower than zero °C which is distinguished from bulk water and it should correspond to the depression phenomenon described above. In the lower-than-threshold level, i.e., the water of fraction (i), the molecules of water interact with polar functional groups such as carboxyl groups on polymer chains. The interaction would be well-oriented hydrogen bonding which is locally favorable configuration that being strong enough to prevent water to form ice crystals (Ping, et al., 2001). The differential scanning calorimetric (DSC) study can reveal the freezable water fractions, for example: Nakamura et al. (1981) reported two DSC peaks of crystallization of absorbed water on celluloses including a broad peak observed at ~230-250 K and a sharp one at ~255 K. Should the melting depression of water of fraction (ii) be due to polymer-water interaction, the corresponding DSC peak then could describe the thermodynamics of a polymer-water system. Many techniques are available for the experimental determination of the interaction parameter between solvent molecules and the polymeric chain segment. However, the methods were usually based on volumetric determinations (Mantovani, et al., 2000). The melting/freezing depression determined by DSC could also exhibit the great potential to characterize that interaction. The aim of the study is to examine

the thermal behavior of water melting depression due to its interaction with the selected starch and cellulose based polymers commonly used in drug delivery formulations by mean of DSC technique.

2. The thermodynamic relations for a polymer solution

A general thermodynamic theory of polymer solution based on mixing according to liquid lattice theory has been presented by Flory (1971). For polymeric hydrogels employed in the present study, the chemical potential of water (μ_1) in a water-polymer system includes not only Flory's mixing with swollen gel but the Donnan equilibrium for polyelectrolytes that yields the following relationship (Flory, 1971; Okoroafor, et al., 1998; Mantovani, et al., 2000; Ozmen & Okay, 2005; and Borchard, et al., 2005):

$$(1) \qquad \mu_1^{gel} - \mu_1^0 = RT[\ln(1-\varphi_2) + \varphi_2 + \chi_1\varphi_2^2 + V_1(\frac{v_e}{V_0})(\varphi_2^{1/3} - \frac{\varphi_2}{2}) - f\cdot\varphi_2]$$

Where, φ_2, χ_1, v_e, and f are volume fraction of polymer in gel, the Flory's polymer-water interaction parameter, the effective crosslink density of the network, and the fraction of charged units in the hydrogel network, respectively. V_1 and V_0 are molar volume of water and the volume of relaxed hydrogel network. R and T are gas constant and absolute temperature. μ_1^0 is the chemical potential of pure liquid water. And, μ_1^{gel} is the chemical potential of water in hydrogel. The first three terms in the right hand side of equation 1 represent the chemical potential of general polymer-water mixture. The fourth term is the chemical potential due to reaction of the network crosslink structure (Flory, 1971), whereas the last term is that from Donnan equilibrium theory (Mantovani et al. 2000; and Ozmen & Okay, 2005).

It is further assumed that frozen water is in equilibrium with the unfrozen water in gel phase during the DSC operation, i.e., the chemical potential of freezing

ice (μ_1^{ice}) and of water in hydrogel (μ_1^{gel}) must be equal. And when a mixture freezes, one of the colligative properties known as freezing point depression holds. The change of chemical potential can be written as (Ozmen & Okay, 2005):

(2) $$\mu_1^{ice} - \mu_1^0 = \Delta H_m (\frac{T}{T_0} - 1)$$

Where ΔH_m, and T_0 are molar enthalpy of crystallization (or melting), and melting temperature of pure water, respectively. Since the left hand side of equation 1 and 2 are equal, the arrangement of these two equations yields:

(3) $$\frac{1}{T} = \frac{1}{T_0} - \frac{R}{\Delta H_m} \cdot [\ln(1-\varphi_2) + \varphi_2 + \chi_1 \varphi_2^2 + V_1 (\frac{v_e}{V_0})(\varphi_2^{1/3} - \frac{\varphi_2}{2}) - f \cdot \varphi_2]$$

This equation should be applicable to the water of fraction (ii) where the ice-liquid water transition temperature was depressed. And, assuming the involved parameters are constant over the transition temperature, the parameters such as χ_1 could be obtained by non-linear regression of $\frac{1}{T}$ as a function of φ_2 according to the model described by equation 3.

3. Materials and Method

3.1 *Materials*

The variety in nature of starch and cellulose based polymers including pre-gelatinized potato starch (PS: Starch®1500, Colorcon, Inc., PA, USA), sodium alginate (SA: Wendt-Chemie, Hamburg, Germany), sodium starch glycolate (SSG: Explotab®, JRS Pharma, Rosenberg, Germany), hydroxypropyl methyl cellulose (HPMC: Colorcon, Inc., PA, USA), Sodium carboxymethyl cellolose (SCMC: Wendt-Chemie, Hamburg, Germany) and croscarmellose sodium (CCS: Ac-di-sol®, FMC Corp. PA, USA) were employed. SA, PS, and SSG were charged-linear, branch

and linear, and charged-crosslinked polysaccharides, respectively. HPMC, SCMC, and CCS were linear, charged-linear, and charged-crosslinked celluloses, respectively.

3.2 *Sub-ambient differential scanning calorimetric study*

The Perkin-Elmer differential scanning calorimeter (DSC7 with TAC7/DX Thermal analysis controller, Perkin-Elmer Crop., Norwalk, CT, USA) equipped with liquid nitrogen bath set as a cooling accessory was employed. Calibrations with Indium and cyclohexane were carried out for every time which the DSC operation started to ensure the accuracy/precision of the obtained heat of transitions and the corresponding temperatures. An accurately weighed (5-15 mg) sample was placed in tightly sealed aluminum pan (Perkin-Elmer Crop., Norwalk, CT, USA). The samples were subjected to run against an empty pan as a reference. With loading temperature of 25 °C, the analysis program includes 1) cooling from 25 °C to -150 °C at 5.00 °C/min rate, 2) isothermal run at -150 °C for 1 min, and 3) heating from -150 °C to 25 °C at the same rate as cooling step. The distilled water was run to validate the temperature and heat of water crystallization/melting. All of DSC thermograms (cooling or heating traces) were analyzed using Pyris® software (Perkin-Elmer Perkin-Elmer Crop., Norwalk, CT, USA).

The samples were pre-treated with ambient humidity prior to DSC analyses. The ~5 g-samples were equilibrated with 85, 96, and 100% relative humidity (RH) at 30.0±0.2 °C for 10 days. The samples were also fully hydrated by liquid water in excess at the same temperature as those pre-treated with ambient humidity as follows: A 3- to 8-gram sample (equivalent to approximately 10-ml bulk volume) was thoroughly mixed with liquid water to 100 ml in volume. The mixtures were allowed to be still for 1 day. Hydrogels or sediments depending to the nature of water-polymer mixtures were subjected to sub-ambient differential scanning calorimetric study

described above. The total water (W_T) contents of hydrogel/sediment samples were determined using a moisture balance (Metter® LP16 & PM300, Metter-Toledo, Inc., Hightstown, NJ, USA) with heating temperature of 100 °C.

3.3 *The determination of non-freezable water*

The water of fraction (i) was calculated by subtracting the total water content (W_T) by the water content calculated from the amount of heat corresponded to DSC melting traces in sub-ambient temperatures assuming that the area of melting peak of pure water corresponds to the melting enthalpy. So, the heat was converted to the amount of water since it was directly proportional to enthalpy of melting obtained from DSC tracing of distilled water.

3.4 *The determination of polymer volume fraction in liquid water*

The fully hydrated polymer volume fraction (ϕ_{2V}) was obtained from particle size determination in non-swelling and swelling states, as analogous to what was done previously (Mantovani et al., 2000). The size and distribution of each of the polymeric powders were measured by dynamic laser light scattering technique (Mastersizer®/E, Malvern Instruments Ltd., Worcestershire, UK). Alcohol and water were used as non-swelling and swelling media, respectively. ϕ_{2V} was obtained by comparing mean volume diameters according to the equation of $\phi_{2V} = [\overline{d_{al}}/\overline{d_w}]^3$, where $\overline{d_{al}}$ and $\overline{d_w}$ are geometric mean volume diameters of a powdered polymer in alcohol and in water, respectively.

To quantify the polymer volume fraction during ice-liquid phase transition of water denoted by φ_2, it was assumed that only pure water freezes when cooled to freezing point. φ_2 is thus directly proportional to the cumulative partial area under the DSC peak at corresponding T, i.e., $\varphi_2 = \varphi_2^{(i)} - \Lambda \frac{A_T}{P}$. Where, A_T, P, $\varphi_2^{(i)}$, and Λ are

the area under the peak at temperature T, the total area under the peak, the polymer volume fraction with water of fraction (i), and the linear coefficient that makes φ_2 equals φ_{2V} determined by light scattering technique, in which A_T equals P, respectively. $\varphi_2^{(i)}$ was approximated from mole fraction of water of fraction (i) ($x_1^{(i)}$) calculated based on the water content of non-freezable water previously described, i.e., $\varphi_2^{(i)} \approx (1 - x_1^{(i)})$. The φ_2 and its corresponding T were non-linearly fitted into Flory's model using the commercial software (SigmaPlot® 2000, SPSS, Inc.).

4. Results and Discussion

4.1 *In situ water crystallization: the validation of DSC measurement*

The cooling and heating traces revealing water crystallization and melting, respectively, are in Figure 1. There was an exothermic peak of water crystallization (I in Figure 1) occurred at a temperature far below zero °C. Endothermic melting peak (II in Figure 1), on the other hand, started at a normal melting temperature. This inconsistency between freezing and melting curves is commonly observed in fairly slow rate of scanning (1-10 °C/min). It is because the crystallization difficulty causes an exotherm to appear at a temperature lower than normal. It seems that the melting trace could approach an equilibrium ice-water transition better than cooling counterpart as the tracing was close to 0 °C. Table 1 shows the detailed information of water melting (II in Figure 1) compared with the reference (Dean, 1985).

As seen in Table 1, both onset and heat of melting for pure water agree with the values taken from the reference. Very low deviations, i.e., 0.37% and 1.18% deviate from reference values for onset and heat of melting, respectively, are observed. It has been stated that in typical DSC measurement, the mean error at heating/cooling rate of 1-10 °C/min should not exceed 2.5% (Borchard, et al., 2005).

Thus, the method and its conditions could be used to investigate water crystallization/melting with acceptable precision and accuracy.

4.2 *DSC water tracings in the selected hydrophilic polymers and the nature of ice-liquid water transition*

Figure 2 illustrates the tracings of water that could be found in SA, SSG, SCMC, and CCS equilibrated with ambient humidity (85-100% RH). For simplicity, the only tracings of SA-100%RH system are showed. As seen in Figure 2, the freezable water in current study is consistent with previous report (Nakamura et al., 1981). It is then subjected into 2 fractions, i.e., water of fraction (ii) labeled as (I) where freezing/melting happen at a temperature below zero, and that of fraction (iii) labeled as (II) where its transitions are closed to normal melting point. Figure 3 illustrates the DSC freezing traces of CCS with various aqueous level environments including that with liquid water in excess. It is noted that other polymers in this study showed similar patterns. However, the water transition tracings were absent in the cases of PS and HPMC in ambient humidity but fully hydrated samples. PS and HPMC are non-ionic polymers exhibiting less hygroscopic than others. It may be because ionic species and salts could attribute to hydration on polymer they present with and might allow amount of water uptake greater than threshold of non-frozen water to show the DSC tracings of water of fraction (ii) and (iii) in cases of SA, SSG, SCMC, and CCS.

Should the porosity formed by 3-dimentional polymer network govern the freezing/melting point depression, the depressed temperature in various moisture environments of the same polymer which would form similar pore structures might be invariant. Furthermore, if the pores collapse during ice formation, the transition of water of fraction (ii) might be either near or far from that of water of fraction (iii) dependent on the new size of the pores that water occupies after collapsing. As

obviously showed in Figures 3, there are not the cases in the present study. It is observed that the phase transition of water of fraction (ii) always exhibits a pattern as a polymer solution, i.e., the more concentration level of water; the more freezing temperature is depressed. Thus rather than porosity confinement, the freezing temperature may be depressed in accord with polymer-water interaction.

Figure 4 illustrates the endothermic melting traces of SSG with variety of humidity as well as fully hydrated sample. Like freezing exotherms, the melting endotherms of various level of water with polymer samples under study were also in similar patterns. It is observed that the melting of freezable bound water shifts toward the melting of free water. i.e., the two singlet peaks turn to a doublet with increase in water content which is similar to the previous study (Borchard et al., 2005). It may be because water of fraction (ii), during increasing temperature, becoming liquid phase migrates from the vicinity of polymer interaction sites within gel due to hydrogen bonding among water molecules to be in equilibrium again with free water that melt later at a normal melting temperature.

4.3 *Non-freezable bound water*

An attempt at the determination of water of fraction (i) for each of polymer-water systems was made and tabulated in Table 2. The materials under study exhibit the non-freezable water contents of between 9.67% and 26.63% whereas it was previously reported that starches and celluloses exhibited non-freezable bound water contents of 28% (Zhong & Sun, 2005) and 22-25% (Luukkonen, at al., 2001), respectively. McCrystal, et al (1997) estimated the number of moles of non-freezing water per a polymer repeating unit for HPMC gel as approximately 3.8 moles that is corresponding to approximately 10-20% water content dependent on degrees of substitution, while the current study on HPMC is within the range (13.21%, Table 2).

On the other hand, the cross-linked chemically modified starch and cellulose that are more hygroscopic (SSG and CCS) illustrate low level of non-freezable bound water (Table 2). It might be because these materials present more number of ice nuclei, during freezing, that draw more water molecules due to hydrogen bonding to the ice clusters as a process of lowering surface free energy. As a result more portion of freezable water may be detected.

4.4 *The volume fraction of polymeric hydrogels vs. melting depression: non-linear fitting to the Flory's model*

The volume fractions in liquid water ($\varphi_{2\,V}$'s) of fully hydrated polymers under study are tabulated in Table 2. It is noted that $\varphi_{2\,V}$'s of SA and HPMC have been taken from the reference (Mutalik, et al., 2006) since the polymers dissolved in water and alcohol, respectively. φ_{2V}'s of sodium starch glycolates have been previously reported as the numbers between 0.005 and 0.045 (Mantovani, et al., 2000) whereas $\varphi_{2\,V}$ of SSG which is chemically identical is 0.031 (Table 2). In addition, the DSC melting traces yield the endotherms closed to 0 °C compared to the exotherms of freezing traces (Figures 2 and 4). Thus the endothermic melting transition of a fully hydrated polymer is used in order to have an appropriate φ_2.

Each of φ_2-T data sets derived from DSC curves was non-linearly fitted into equation 4 with the restricted conditions that $(R/\Delta H_m) = 1.383 \times 10^{-3}$ K^{-1} and $T_0 =$ 273.15 K (Borchard, et al., 2005). The estimates as well as their standard errors (SE) of parameters including χ_1, network factor ($_{V_1}\frac{v_e}{V_0}$) and f are tabulated in Table 3. It is noted that ionic and/or cross-linking network contribution factor was set as null for uncharged and/or linear polymers, respectively. It was found that the model is successfully applied to φ_2-T data sets with high correlations (r^2: 0.934-0.999, Table 3). It is thus demonstrated that χ_1, charges, and polymer network affect the

crystallization/melting of water that the polymer contains. As see in Table 3, *f*'s of charged polymers are statistically significant from null at α-level of 0.05, so are network factors of cross-linked ones except CCS. *f* reflects the degree of ionization whereas network factor illustrates swelling of the cross-linked polymers (Borchard, et al., 2005; Mantovani, et al., 2000). It is observed that at 0.05-α-level, network factor in the case of CCS is not significantly different from null. It might evidently be because the swelling of the polymeric network is not sufficient to significantly effect on the water crystallization / melting for it was previously reported that the swelling capacity of CCS present in water was far lower than that of SSG (Visavarungroj & Remon, 1990). In addition, Okoroafor, et al. (1998) mentioned that the effect of network factor was quite small since its value usually is of the order of two decimal digits. That is consistent with the current study as it is observed that the estimates of network factor are in the same order of magnitude (Table 3).

4.5 *Flory's interaction parameter* (χ_1)

To characterize the thermodynamic interaction between water and polymer, Flory (1971) introduced a dimensionless quantity: χ_1. It represents merely the difference in energy divided by thermal agitation energy (kT: where k is Boltzmen's constant) of a solvent molecule immersed in the pure polymer compared with one surrounded by molecules of its own kind. A number of authors reported the magnitudes of χ_1 of aqueous polymeric solutions including starches and its derivatives (Baks, et al., 2007; Cruz-Orea, et al., 2002; Mantovani, et al., 2000; Farhat & Blanshard, 1997), and sodium alginate (Borchard, et al., 2005) as the numbers ranging between 0.43 and 0.67. As seen in Table 3, the estimates of χ_1-parameters of the same types of polymers vary between 0.520 and 0.761 which are comparable. Myagkova, et al. (1997) mentioned that the χ_1 should be approximately 0.5 for

maximum dissolving capacity of liquid water, i.e., the good-solvent conditions, for cellulose esters whereas the magnitudes of χ_1 for the same type of polymers under study are 0.679-0.847 which also approaches those conditions. In fact, the magnitude χ_1 is somewhat empirical and not a constant. It is dependent on volume fraction as well as temperature (Myagkova, et al.; 1997 and Flory, 1971). Thus experimental conditions should affect its magnitude especially during the initial setting causing χ_1 values to deviate from laboratories to laboratories.

Figure 5 illustrates the plot of χ_1 versus the reciprocal absolute temperature of the onset of DSC melting transition of water of fraction (ii) in fully hydrated samples. It is observed that the smaller the value of χ_1, the larger solvent water melting was depressed, i.e., stronger affinity for water. Flory (1971) rectified the energy quantity of χ_1 that should be regarded as the free energy change rather than as the heat of mixing only. χ_1 then contains an entropy contribution in addition to enthalpy one. Thus, in a simple case (Borchard, et al., 2005):

$$\chi_1 = \alpha_1 + \frac{\beta_1}{T} \quad (4)$$

where, α_1 and β_1 are entropy and enthalpy parameters, respectively. Assuming the same type of interaction, χ_1 derived from polymeric hydrogels in this study could exhibit the relationship with $1/T$ as showed by Equation 4. As seen in Figure 5, the trend line as well as 95% confidence interval (dotted lines in Figure 5) represents the data fitting of Equation 4. Unfortunately, the power of regression and the correlation coefficient are as low as 25.01% and 0.631, respectively. It might be because the variety in nature of individual polymers and experimental conditions could complicate the systems resulting the fitted parameters are so empirical that they are meaningless to address.

Acknowledgement

The authors would like to thank Thailand Research Fund for financial support.

Special thanks also go to the Scientific Equipment Center, Prince of Songkla University; Faculty of Pharmaceutical Sciences' Research and Development Unit; and the Department of Pharmaceutical Technology, Faculty of Pharmaceutical Sciences, Prince of Songkla University for providing the lab facilities.

References

Baks, T., Ngene, I. S., van Soest, J. J. G., Janssen, A. E. M., Boom, R. M. 2007. Comparison of methods to determine the degree of gelatinisation for both high and low starch concentrations. *Carbohyd. Polym*. 67: 481-490.

Borchard, W., Kenning, A., Kapp, A., Mayer, C. 2005. Phase diagram of the system sodium alginate/water: A model for biofilms. *Int. J. Biol. Macromole*. 35: 247-256.

Dean, J. A., 1985. Lange's Handbook of chemistry, 13rd Ed., McGraw-Hill, New York, p. 9-117.

Faroongsarng, D., Peck, G. E. 2003. Thermal porosity analysis of croscarmellose sodium and sodium Starch Glycolate by differential scanning calorimetry. *AAPSPharmSciTech*. 4(4): article 67.

Flory, P. J. 1971. *Principles of polymer chemistry*. Cornell University Press, Ithaca and London.

Hay, J. N., Laity, P. R. 2000. Observation of water migration during thermoporometry studies of cellulose films. *Polymer*. 41: 6171-6180.

Higuchi, A., Iijima, T. 1985. DSC investigation of the states of the water in poly(vinyl alcohol) membranes. *Polymer*. 26: 1207-1211

Ilmain, F., Tanaka, T., Kokufuta, E. 1991. Volume transition in a gel driven by hydrogen bonding. *Nature*. 349: 400-401.

Ishikiriyama, K., Todoki, M. 1995. Pore size distribution measurements of silica gels by means of differential scanning calorimetry. *J. Colloid Interf. Sci.* 171: 103-111.

Luukkonen, P., Maloney, T., Rantanen, J., Paulapuro, H., Yliruusi, J. 2001. Microcrystalline cellulose-water interaction-A novel approach using thermoporosimetry. *Pharm. Res*. 18(11): 1562-1569.

Mantovani, F., Grassi, M., Colombo, I., Lapasin, R. 2000. A combination of vapor sorption and dynamic laser light scattering methods for the determination of the parameter χ and the crosslimk density of a powdered polymeric gel. *Fluid Phase Equilibr*. 167: 63-81.

McCrystal, C. B, Ford, J. L., Rajabi-Siahboomi, A. R. 1997. A study on the interaction of water and cellulose ethers using differential scanning calorimetry. *Thermochim. Acta*. 294: 91-98.

Mutalik, V., Manjeshwar, L. S., Wali, A., Sairam, M., Raju, K. V. S. N., Aminabhavi, T. M. 2006. Thermodynamics/hydrodymanics of aqueous polymer solutions and dynamic mechanical characterization of solid films of chitosan, sodium alginate, guar gum, hydroxyl ethyl cellulose and hydroxypropyl methylcellulose at different temperatures. *Carbohyd. Polym*. 65: 9-21.

Myagkova, N. V., Rakhmonberdiev, G. R., Sagdieva, Z. G., Sidikov, A. S. 1997. Thermodynamic properties of solutions of water-soluble mixed cellulose esters. *Chem. Nat. Compd*. 33(1): 76-79.

Nakamura, K., Hatakeyama, T., Hatakeyama, H. 1981. Studies on bound water of cellulose by differential scanning calorimetry. *Tex. Res. J*. 51(9): 607-613.

Okoroafor, E. U., Newborough, M., Highgate, D., Augood, P. 1998. The thermal behaviour of water in crosslinked hydro-active polymeric structure: crystasllization of water. *J. Phys. D: Appl. Phys*. 31: 3120-3129.

Ozmen, M. M., Okay, O. 2005. *Polymer*. 46: 8119-8127.

Ping, Z. H., Nguyen, Q. T., Chen, S.M., Zhou, J. Q., Ding, Y. D. 2001. States of water in different hydrophilic polymers-DSC and FTIR studies. *Polymer*. 42: 8461-8467.

Rajabi-Siahboomi, A. R., Bowtell, R. W., Mansfield, P., Davies, M. C., Melia, C. D. 1996. Structure and Behavior in Hydrophilic Matrix Sustained Release Dosage Forms: 4. Studies of Water Mobility and Diffusion Coefficients in the Gel Layer of HPMC Tablets Using NMR Imaging. *Pharm Res*. 13(3): 376-380.

Rault, J., Gref, R., Ping, Z. H., Nguyen, Q. T., Neel, J. 1995. *Polymer*. 36: 1655-31.

Visavarungroj N, Remon J P. 1990. Crosslinked starch as a disintegrating agent. *Int. J. Pharm*. 62: 125-131.

Yamamoto, T., Mukai, S.R., Nitta, K., Tamon, H., Endo, A., Ohmori, T., Nakaiwa, M. 2005. Evaluation of porous structure of resorcinol-formaldehyde hydrogels by thermoporometry. *Thermochim. acta*. 439: 74-79.

Zhong, Z., Sun, X. S. 2005. Thermal characterization and phase behavior of cornstarch studied by differential scanning calorimetry. *J. Food Eng*. 69: 453-459.

Zografi, G., Kontny, M. J. 1986. The interactions of water with cellulose- and starch-derived pharmaceutical excipients. *Pharm. Res*. 3(4): 187-194.

Parameter	DSC run	Reference (1)	Deviation (%)
Onset; Peak (K)	274.15; 275.4	273.15	+0.37; +0.82
Heat of melting (Kcal/mol)	1.453	1.436	+1.18

Table 1.Water melting information taken from endotherm (heating trace) compared with the reference (Dean, 1985).

Polymeric material	[1]Overall water content (%)	[2]Freezable water content (%) (mean, s.d.)	[3]Water of fraction (i) (%)	[4] φ_{2V}
PS	80.01	53.38, 1.09	26.63	0.112
SA	73.36	47.43, 1.07	25.93	[a]0.167
SSG	73.28	52.30, 1.11	20.98	0.031
HPMC	51.30	38.09, 0.87	13.21	[a]0.384
SCMC	69.13	46.14, 0.78	22.99	0.145
CCS	79.97	70.30, 1.11	9.67	0.054

1. Overall water content was determined by moisture balance.
2. Freezable water content was determined by DSC traces calculation (in 3 replicates) based on the heat of melting in Table 1.
3. Non-freezable water content was calculated as Overall water content minus Freezable water content.
4. The fully hydrated polymer volume fraction based on equation (Mantovani et al., 2000): $\phi_{2V} = [\overline{d_{al}}/\overline{d_w}]^3$ where $\overline{d_{al}}$ and $\overline{d_w}$ are geometric mean volume diameters of a powdered polymer in alcohol and in water, respectively.

a. The numbers are taken from reference (Mutalik et al., 2006) since the equipment could not determine.

Table 2. Water contents and the volume fractions of fully hydrated hydrophilic polymers under study.

Polymeric material	χ_1 Estimate, SE	$V_1\frac{v_e}{V_0}$ Estimate, SE	f Estimate, SE	r^2
PS	0.761, 0.041	0.067, 0.017	**-	0.939
SA	0.738, 0.033	*-	0.513, 0.022	0.986
SSG	0.520, 0.051	0.084, 0.010	0.288, 0.093	0.994
HPMC	0.847, 0.032	*-	**-	0.934
SCMC	0.776, 0.021	*-	0.368, 0.070	0.947
CCS	0.679, 0.025	[a] 0.028, 0.048	0.241, 0.002	0.999

* Since the polymers are linear, network contribution is absent.
**Since the polymers are uncharged, the reduced model with $f = 0$ is used.
[a] The contribution is statistically non-significant at 0.05 α-level.

Table 3. The estimates of the parameters according to the restricted ($R/\Delta H_m = 1.383 \times 10^{-3}$ K^{-1} and $T_0 = 273.15$ K) non-linear regression of equation 3.

Figure legends

Figure 1. DSC thermograms of water illustrating water crystallization (cooling trace: I) and melting (heating trace: II). DSC was done according to the conditions listed in Table 1.

Figure 2. DSC thermograms (cooling [A] and heating [B] curves) of SA previously equilibrated in 100%RH at 30 degrees C for 7 days showing 2 phases of water on a polymer surface. (I) is freezable bound water and (II) is bulk water.

Figure 3. DSC freezing traces of water in the samples of CCS equilibrated with (a) 96% RH, (b) 100%RH, and (c) liquid water. It is noted that hydrogels of other polymer under study also exhibit similar behavior.

Figure 4. DSC endothermic melting of ice in SSG equilibrated with (a) 84% RH, (b) 96% RH, (c) 100% RH, and (d) excess liquid water (fully hydrated). It is noted that hydrogels of other polymer under study also exhibit similar behavior.

Figure 5. The plot of χ_1-parameter against the reciprocal of onset temperature (in absolute scale) of melting transition of freezable bound water in water-polymer systems under study.

Figure 1
Click here to download high resolution image

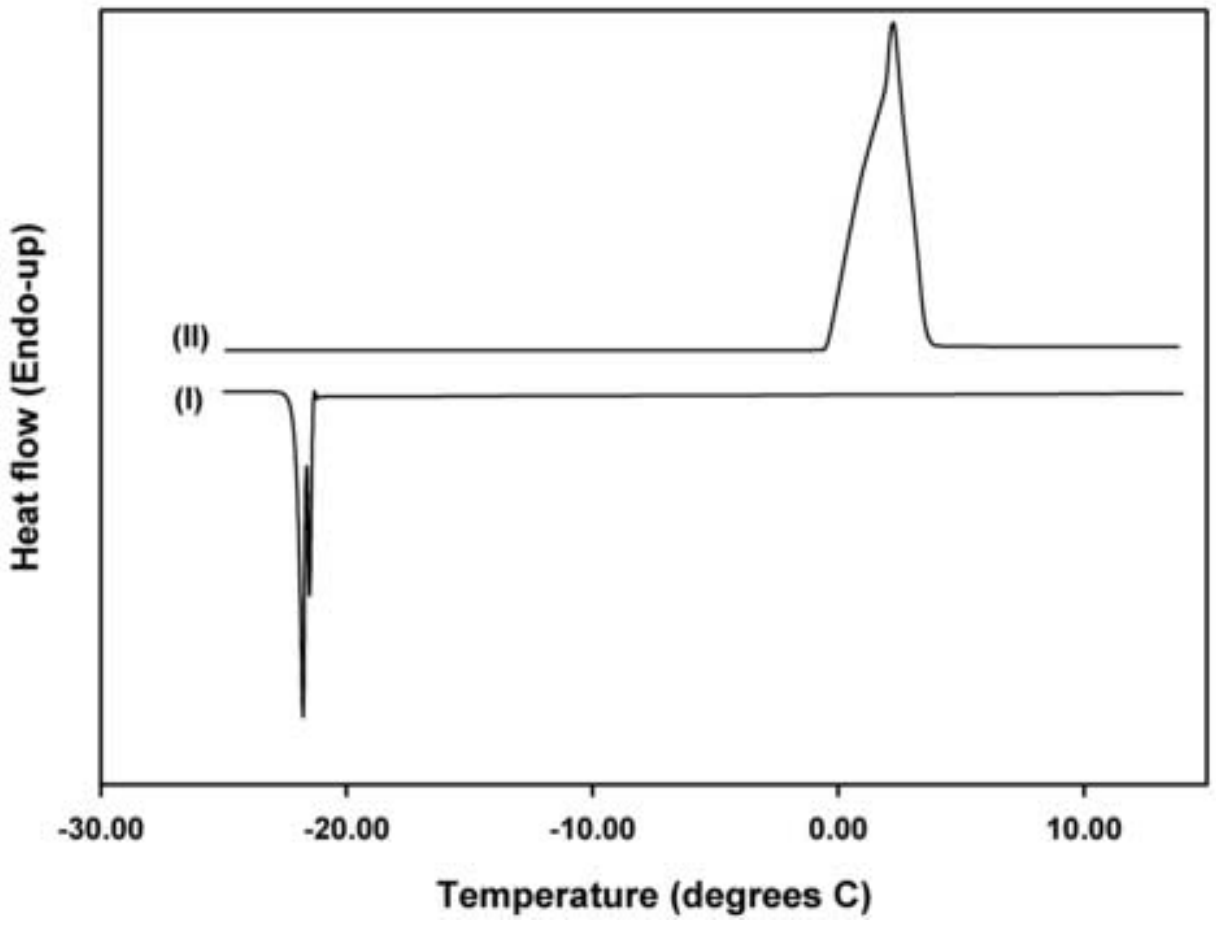

Figure 2
Click here to download high resolution image

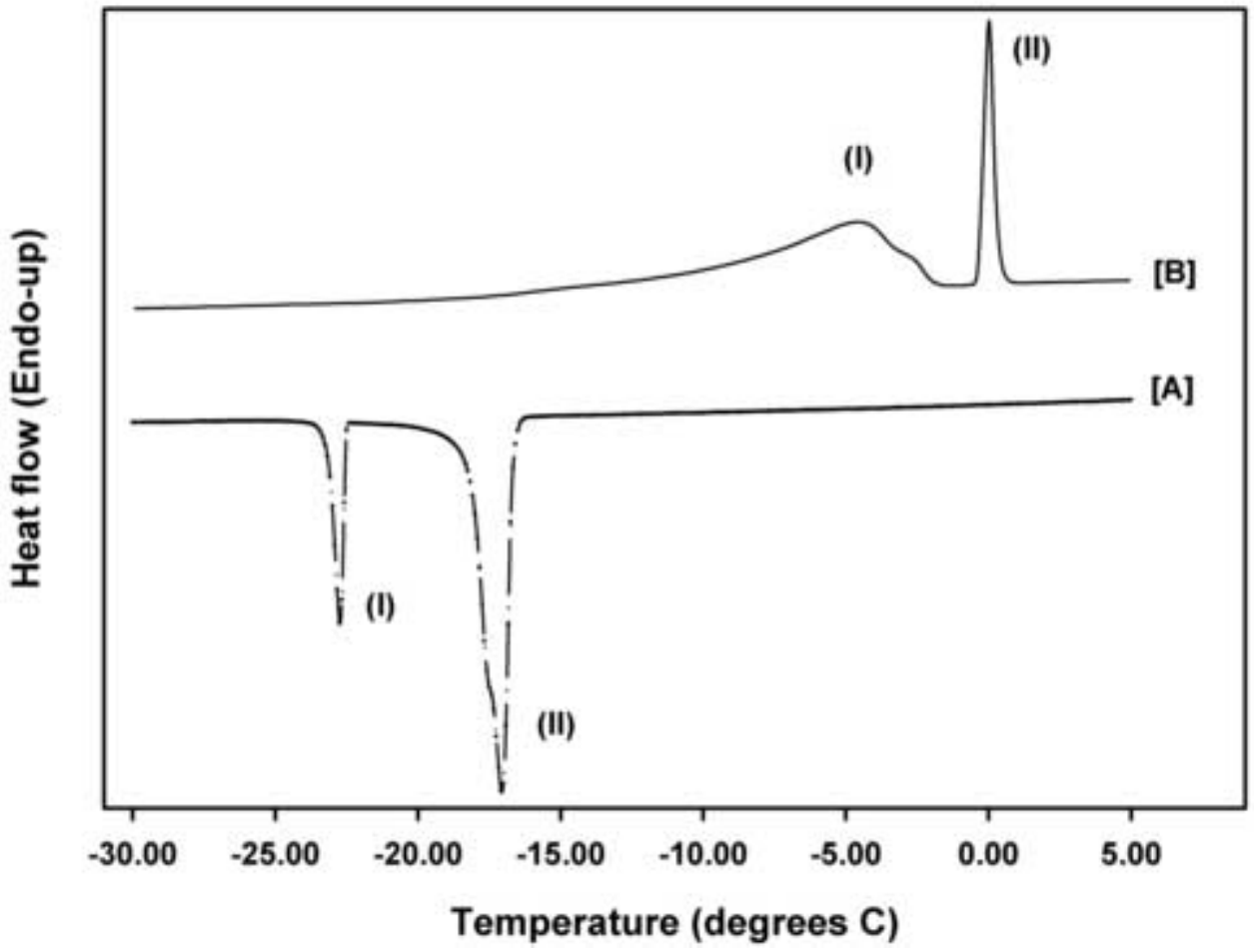

Figure 3
Click here to download high resolution image

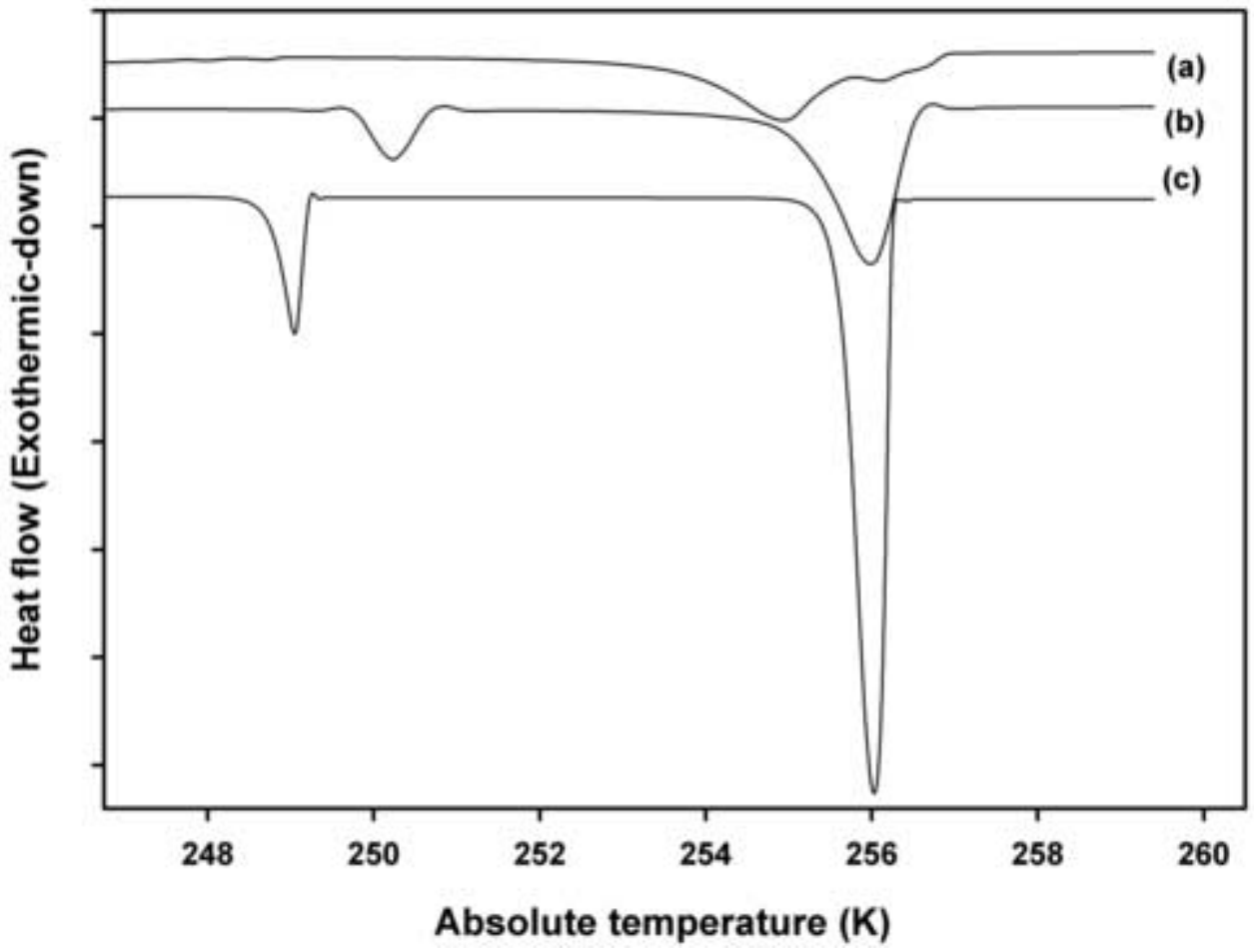

Figure 4
Click here to download high resolution image

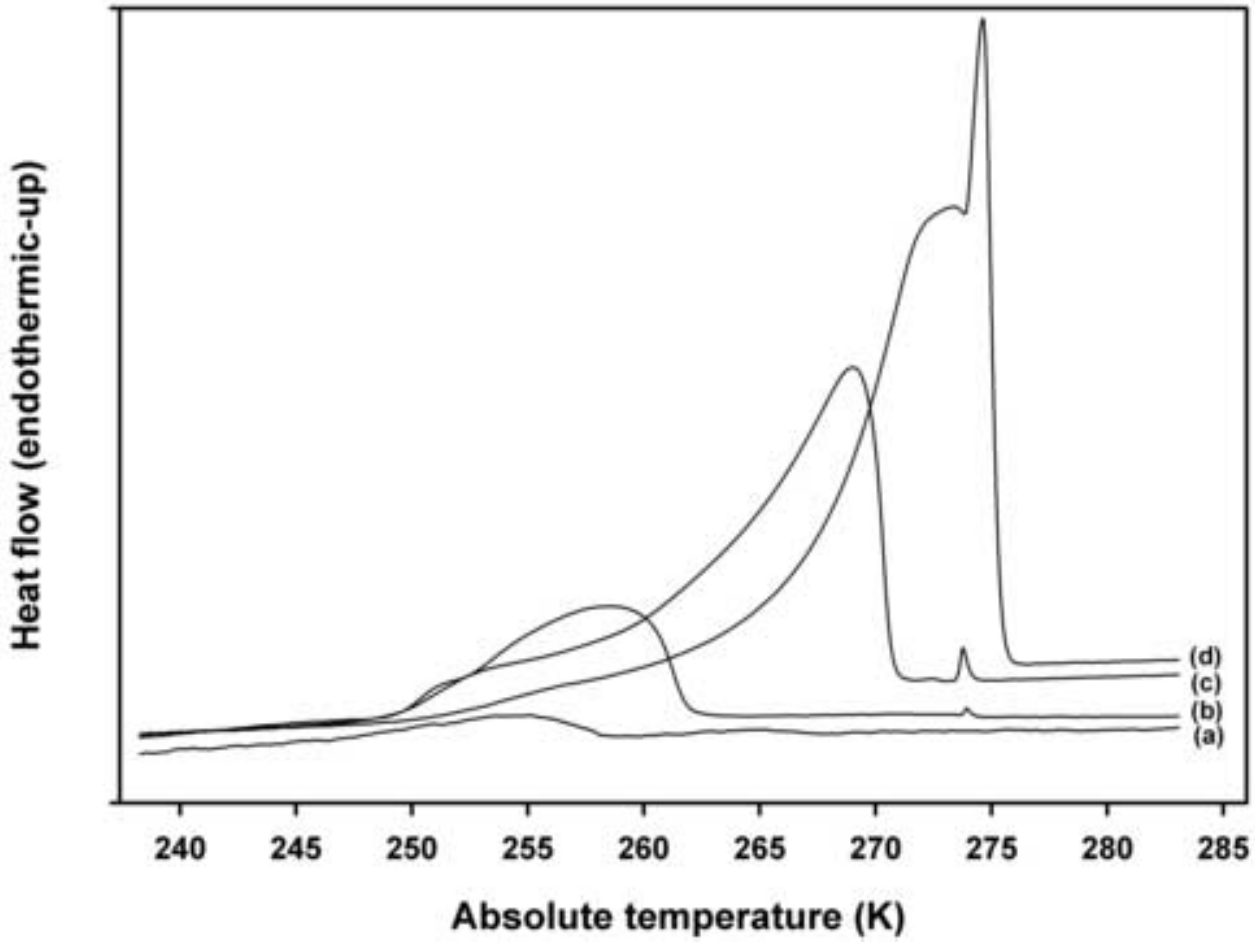

Figure 5
Click here to download high resolution image

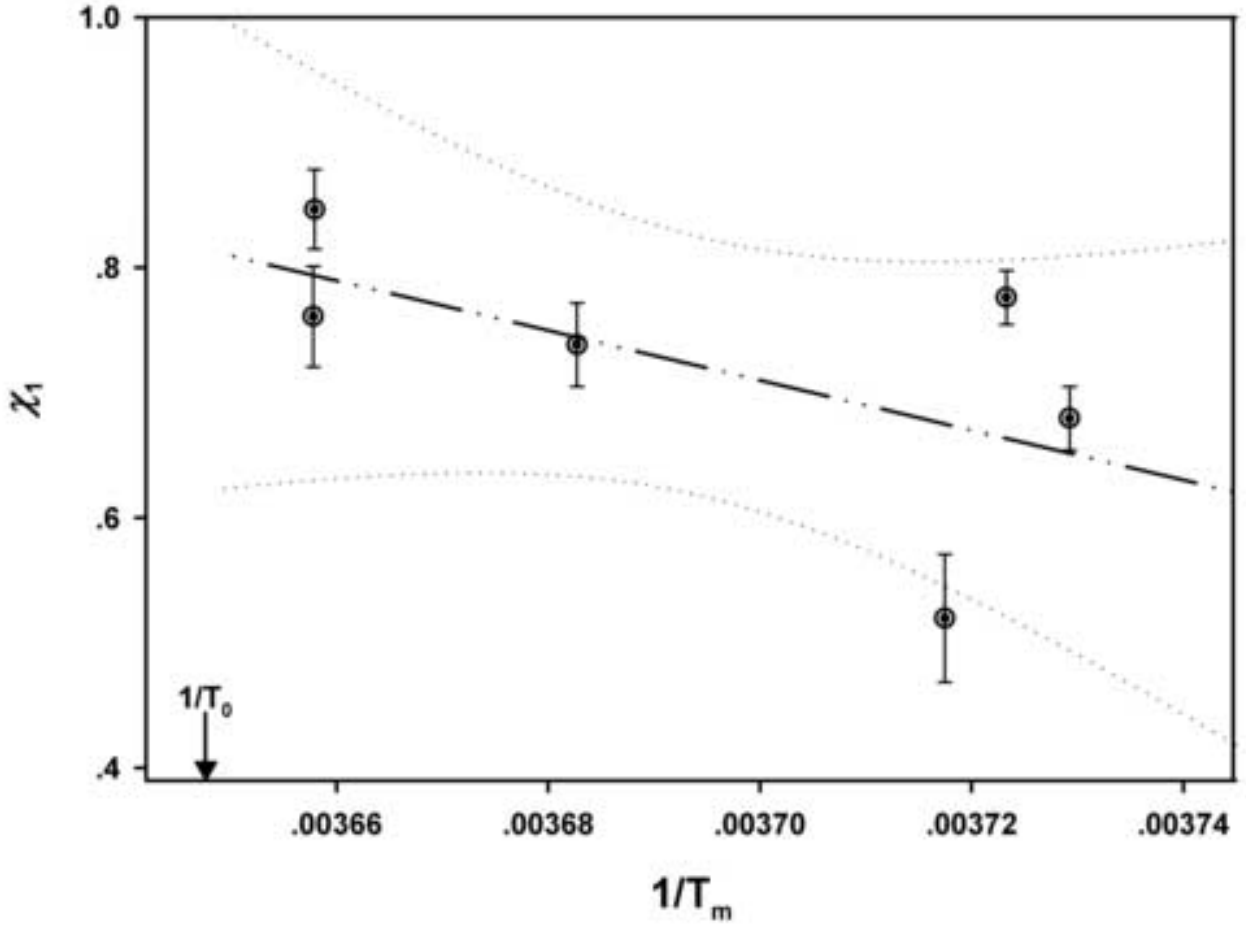

Output ที่ได้จากโครงการ

Faroongsarng, D., and Sukonrat, P. Thermal behavior of water in polymeric hydrogels of the selected pharmaceutical excipients. *Int. J. Pharm*. Submitted and under review.

Elsevier Editorial System(tm) for International Journal of Pharmaceutics

Manuscript Draft

Manuscript Number: IJP-D-07-00617

Title: Thermal behavior of water in polymeric hydrogels of the selected pharmaceutical excipients

Article Type: Research Paper

Section/Category:

Keywords: freezable water, water-polymer interaction, Flory's interaction parameter (χ1), melting point depression, hydrogel

Corresponding Author: Associate Professor Damrongsak - Faroongsarng, Ph.D.

Corresponding Author's Institution: Prince of Songkla University

First Author: Damrongsak - Faroongsarng, Ph.D.

Order of Authors: Damrongsak - Faroongsarng, Ph.D.; Patchara - Sukonrat

Abstract: In a polymer-water matrix, freezable water is depressed due to either porosity confinement or interaction. The aim of the study was to examine water crystallization/melting depression by sub-ambient differential scanning calorimetry. The selected starch and cellulose based excipients including pre-gelatinized starch (PS), sodium alginate, sodium starch glycolate, hydroxypropylmethyl cellulose (HPMC), sodium carboxymethyl cellulose, and croscarmellose sodium were employed. The pre-treated with ambient humidity (85-100% relative humidity, at 30.0±0.2°C for 10 days) and with excess water (hydrogels) samples were subjected to a 25 - -150°C-cooling-heating cycle at 5.00 °C/min rate. The volume fractions of hydrogels were measured by light scattering technique. It was observed that all polymers but PS and HPMC with ambient humidity presented freezable water in two distinct fractions namely bound water where crystallizing/melting temperature was depressed and bulk water. The water transition in samples with various contents exhibited the pattern as a polymer solution, thus rather than confinement, the depression was due to interaction. The volume fraction-melting temperature data derived from endotherms of hydrogels were successfully fitted to Flory's model (r2: 0.934-0.999). The Flory's interaction parameters (χ1) were found to vary between 0.520 and 0.847. In addition, the smaller the value of χ1, the larger melting was depressed, i.e., stronger affinity for water.

were successfully fitted to Flory's model (r2: 0.934-0.999). The Flory's interaction parameters ($\chi 1$) were found to vary between 0.520 and 0.847. In addition, the smaller the value of $\chi 1$, the larger melting was depressed, i.e., stronger affinity for water.

*** Letter of Submission**

Faculty of Pharmaceutical Sciences
Department of Pharmaceutical Technology
Prince of Songkla University, Hat Yai, Thailand 90112.

June 13, 2007

Dear Editor:

I would like to submit the manuscript entitled: "Thermal behavior of water in polymeric hydrogels of the selected pharmaceutical excipients" to *Int. J. Pharm*. The manuscript describes the crystallization/melting depression of water present in hydrogels of various polymeric pharmaceutical excipients used in drug delivery dosage forms that could be detected by differential scanning calorimetry. We derived the information from DSC tracings and the obtained information was successfully modeled using Flory's polymer solution theory.

Although the DSC technique is not new, the manuscript could provide the novel insight into the thermodynamic principles of polymer-water interaction.

Sincerely,

Damrongsak Faroongsarng, Ph.D.

IJP AUTHOR CHECKLIST

Dear Author,

It frequently happens that on receipt of an article for publication, we find that certain elements of the manuscript, or related information, is missing. This is regrettable of course since it means there will be a delay in processing the article while we obtain the missing details.

In order to avoid such delays in the publication of your article, if accepted, could you please run through the list of items below and make sure you have completed the items.

Overall Manuscript Details

- Is this the final revised version? ☑
- Are all text pages present? ☑
- Are the corresponding author's postal address, telephone and fax numbers complete on the manuscript? ☑
- **Have you provided the corresponding author's e-mail address?** ☑
- **Manuscript type – please check one of the following:**
  - Full-length article ☑
  - Review article ☐
  - Rapid Communication ☐
  - Note ☐
  - Letter to the Editor ☐
  - Other ☐
- **Manuscript section – paper to be published in:**
  - Pharmaceutical nanotechnology section ☐

Manuscript elements

- Short summary/abstract enclosed? ☑
- 3-6 Keywords enclosed? ☑
- Complete reference list enclosed? ☑
- Is the reference list in the correct journal style? ☑
- Are all references cited in the text present in the reference list? ☑
- Are all **original** figures cited in the text enclosed? ☑
  Electronic artwork format? ----------
- Are figure legends supplied? ☑
- Are all figures numbered and orientation provided? ☑
- Are any figures to be printed in colour? ☐
  If yes, please list which figures here:----------
- If applicable, are you prepared to pay for reproduction in colour? ☐
- Are all tables cited in the text supplied? ☑

General

- Can you accept pdf proofs sent via e-mail? ☑

*** Manuscript**

Title: Thermal behavior of water in polymeric hydrogels of the selected pharmaceutical excipients

Authors and affiliations:

*Damrongsak Faroongsarng
Drug Delivery Systems Research Center, Department of Pharmaceutical Technology, Faculty of Pharmaceutical Sciences, Prince of Songkla University, Hat Yai 90112, Thailand.

Patchara Sukonrat
Scientific Equipment Center, Prince of Songkla University, Hat Yai, 90112, Thailand.

*Corresponding author
e-mail: damrongsak.f@psu.ac.th
Phone: +66-74-288-841
FAX: +66-74-428-148

Thermal behavior of water in polymeric hydrogels of the selected pharmaceutical excipients

Abstract

In a polymer-water matrix, freezable water is depressed due to either porosity confinement or interaction. The aim of the study was to examine water crystallization/melting depression by sub-ambient differential scanning calorimetry. The selected starch and cellulose based excipients including pre-gelatinized starch (PS), sodium alginate, sodium starch glycolate, hydroxypropylmethyl cellulose (HPMC), sodium carboxymethyl cellulose, and croscarmellose sodium were employed. The pre-treated with ambient humidity (85-100% relative humidity, at 30.0±0.2°C for 10 days) and with excess water (hydrogels) samples were subjected to a 25 - -150°C-cooling-heating cycle at 5.00 °C/min rate. The volume fractions of hydrogels were measured by light scattering technique. It was observed that all polymers but PS and HPMC with ambient humidity presented freezable water in two distinct fractions namely bound water where crystallizing/melting temperature was depressed and bulk water. The water transition in samples with various contents exhibited the pattern as a polymer solution, thus rather than confinement, the depression was due to interaction. The volume fraction-melting temperature data derived from endotherms of hydrogels were successfully fitted to Flory's model (r^2: 0.934-0.999). The Flory's interaction parameters (χ_1) were found to vary between 0.520 and 0.847. In addition, the smaller the value of χ_1, the larger melting was depressed, i.e., stronger affinity for water.

Keywords: freezable water, water-polymer interaction, Flory's interaction parameter (χ_1), melting point depression, hydrogel.

1. Introduction

Starch and cellulose based materials derived from naturally occur biopolymers are the major pharmaceutical excipients utilized in drug delivery dosage forms. These polymers always interact with water due to their hydrophilicity exhibiting some properties that may critically affect the dosage form performance. For example: In controlled release devices, water diffusion through a polymeric hydrogel layer has been considered as one of the major factors determining drug release rate (Rajabi-Siahboomi, et al., 1996). With liquid water in excess, these hydrophilic polymers could form hydrogels i.e., the three-dimensional arrangement possessing the ability to retain a significant fraction of water without complete dissolving. A hydrogel might form relatively stable space lattice or network pores fulfilled with a considerable amount of water. The interfacial tension related to surface of curvature of water within pores could develop and affect the phase transition of the water. Thus this phase transition of water confinement could somehow characterize the pores where it occupies. A number of authors, for examples: Yamamoto at al. (2005), Faroongsarng & Peck (2003), Hay & Laity (2000), and Ishikiriyama & Todoki (1995) examined the pore sizes and distributions of various porous materials assuming that water is mostly held within pores, with melting temperature being depressed by Gibbs-Thomson effect. However, the depression of melting temperature is not only attributed by water confinement in porosity but the water-polymer interaction. Rault et al (1994) reported that the melting depression and the concentration of unfrozen water varied with the water concentration with similar orders of magnitude for polymer-water systems and simple binary mixtures, presenting the same type of interaction, from which confinement effects are absent. They concluded that the melting depression is due not to water confinement in polymer network porosity but rather to water-polymer interactions. The evidence was later confirmed by the work of Okoroafor et al (1998).

In general, interactions between macromolecules fall into four categories: ionic, hydrophobic, van der Waals and hydrogen bonding (Ilmain, et al., 1991). But for a polymer-water mixture, the interaction is always in the range of hydrogen bonding. It has been proposed (Ping, et al., 2001; Zografi & Kontny, 1986; and Higuchi & Iijima, 1985) that water in hydrophilic polymer matrices presents in three distinct fractions: (i) non-freezable bound water, (ii) freezable bound water, and (iii) free or bulk water. Upon cooling, water begins to crystallize only when its content is above a characteristic threshold. This fraction of water has been called freezable bound water (fraction (ii)) because it exhibits a melting point lower than zero °C which is distinguished from bulk water and it should correspond to the depression phenomenon described above. In the lower-than-threshold level, i.e., the water of fraction (i), the molecules of water interact with polar functional groups such as carboxyl groups on polymer chains. The interaction would be well-oriented hydrogen bonding which is locally favorable configuration that being strong enough to prevent water to form ice crystals (Ping, et al., 2001). The differential scanning calorimetric (DSC) study can reveal the freezable water fractions, for example: Nakamura et al. (1981) reported two DSC peaks of crystallization of absorbed water on celluloses including a broad peak observed at ~230-250 K and a sharp one at ~255 K. Should the melting depression of water of fraction (ii) be due to polymer-water interaction, the corresponding DSC peak then could describe the thermodynamics of a polymer-water system. Many techniques are available for the experimental determination of the interaction parameter between solvent molecules and the polymeric chain segment. However, the methods were usually based on volumetric determinations (Mantovani, et al., 2000). The melting/freezing depression determined by DSC could also exhibit the great potential to characterize that interaction. The aim of the study is to examine

the thermal behavior of water melting depression due to its interaction with the selected starch and cellulose based polymers commonly used in drug delivery formulations by mean of DSC technique.

2. The thermodynamic relations for a polymer solution

A general thermodynamic theory of polymer solution based on mixing according to liquid lattice theory has been presented by Flory (1971). For polymeric hydrogels employed in the present study, the chemical potential of water (μ_1) in a water-polymer system includes not only Flory's mixing with swollen gel but the Donnan equilibrium for polyelectrolytes that yields the following relationship (Flory, 1971; Okoroafor, et al., 1998; Mantovani, et al., 2000; Ozmen & Okay, 2005; and Borchard, et al., 2005):

$$(1) \qquad \mu_1^{gel} - \mu_1^0 = RT[\ln(1-\varphi_2) + \varphi_2 + \chi_1\varphi_2^2 + V_1(\frac{v_e}{V_0})(\varphi_2^{1/3} - \frac{\varphi_2}{2}) - f\cdot\varphi_2]$$

Where, φ_2, χ_1, v_e, and f are volume fraction of polymer in gel, the Flory's polymer-water interaction parameter, the effective crosslink density of the network, and the fraction of charged units in the hydrogel network, respectively. V_1 and V_0 are molar volume of water and the volume of relaxed hydrogel network. R and T are gas constant and absolute temperature. μ_1^0 is the chemical potential of pure liquid water. And, μ_1^{gel} is the chemical potential of water in hydrogel. The first three terms in the right hand side of equation 1 represent the chemical potential of general polymer-water mixture. The fourth term is the chemical potential due to reaction of the network crosslink structure (Flory, 1971), whereas the last term is that from Donnan equilibrium theory (Mantovani et al. 2000; and Ozmen & Okay, 2005).

It is further assumed that frozen water is in equilibrium with the unfrozen water in gel phase during the DSC operation, i.e., the chemical potential of freezing

ice (μ_1^{ice}) and of water in hydrogel (μ_1^{gel}) must be equal. And when a mixture freezes, one of the colligative properties known as freezing point depression holds. The change of chemical potential can be written as (Ozmen & Okay, 2005):

(2) $$\mu_1^{ice} - \mu_1^0 = \Delta H_m (\frac{T}{T_0} - 1)$$

Where ΔH_m, and T_0 are molar enthalpy of crystallization (or melting), and melting temperature of pure water, respectively. Since the left hand side of equation 1 and 2 are equal, the arrangement of these two equations yields:

(3) $$\frac{1}{T} = \frac{1}{T_0} - \frac{R}{\Delta H_m} \cdot [\ln(1-\varphi_2) + \varphi_2 + \chi_1 \varphi_2^2 + V_1 (\frac{v_e}{V_0})(\varphi_2^{1/3} - \frac{\varphi_2}{2}) - f \cdot \varphi_2]$$

This equation should be applicable to the water of fraction (ii) where the ice-liquid water transition temperature was depressed. And, assuming the involved parameters are constant over the transition temperature, the parameters such as χ_1 could be obtained by non-linear regression of $\frac{1}{T}$ as a function of φ_2 according to the model described by equation 3.

3. Materials and Method

3.1 *Materials*

The variety in nature of starch and cellulose based polymers including pre-gelatinized potato starch (PS: Starch®1500, Colorcon, Inc., PA, USA), sodium alginate (SA: Wendt-Chemie, Hamburg, Germany), sodium starch glycolate (SSG: Explotab®, JRS Pharma, Rosenberg, Germany), hydroxypropyl methyl cellulose (HPMC: Colorcon, Inc., PA, USA), Sodium carboxymethyl cellolose (SCMC: Wendt-Chemie, Hamburg, Germany) and croscarmellose sodium (CCS: Ac-di-sol®, FMC Corp. PA, USA) were employed. SA, PS, and SSG were charged-linear, branch

and linear, and charged-crosslinked polysaccharides, respectively. HPMC, SCMC, and CCS were linear, charged-linear, and charged-crosslinked celluloses, respectively.

3.2 *Sub-ambient differential scanning calorimetric study*

The Perkin-Elmer differential scanning calorimeter (DSC7 with TAC7/DX Thermal analysis controller, Perkin-Elmer Crop., Norwalk, CT, USA) equipped with liquid nitrogen bath set as a cooling accessory was employed. Calibrations with Indium and cyclohexane were carried out for every time which the DSC operation started to ensure the accuracy/precision of the obtained heat of transitions and the corresponding temperatures. An accurately weighed (5-15 mg) sample was placed in tightly sealed aluminum pan (Perkin-Elmer Crop., Norwalk, CT, USA). The samples were subjected to run against an empty pan as a reference. With loading temperature of 25 °C, the analysis program includes 1) cooling from 25 °C to -150 °C at 5.00 °C/min rate, 2) isothermal run at -150 °C for 1 min, and 3) heating from -150 °C to 25 °C at the same rate as cooling step. The distilled water was run to validate the temperature and heat of water crystallization/melting. All of DSC thermograms (cooling or heating traces) were analyzed using Pyris® software (Perkin-Elmer Perkin-Elmer Crop., Norwalk, CT, USA).

The samples were pre-treated with ambient humidity prior to DSC analyses. The ~5 g-samples were equilibrated with 85, 96, and 100% relative humidity (RH) at 30.0±0.2 °C for 10 days. The samples were also fully hydrated by liquid water in excess at the same temperature as those pre-treated with ambient humidity as follows: A 3- to 8-gram sample (equivalent to approximately 10-ml bulk volume) was thoroughly mixed with liquid water to 100 ml in volume. The mixtures were allowed to be still for 1 day. Hydrogels or sediments depending to the nature of water-polymer mixtures were subjected to sub-ambient differential scanning calorimetric study

described above. The total water (W_T) contents of hydrogel/sediment samples were determined using a moisture balance (Metter® LP16 & PM300, Metter-Toledo, Inc., Hightstown, NJ, USA) with heating temperature of 100 °C.

3.3 *The determination of non-freezable water*

The water of fraction (i) was calculated by subtracting the total water content (W_T) by the water content calculated from the amount of heat corresponded to DSC melting traces in sub-ambient temperatures assuming that the area of melting peak of pure water corresponds to the melting enthalpy. So, the heat was converted to the amount of water since it was directly proportional to enthalpy of melting obtained from DSC tracing of distilled water.

3.4 *The determination of polymer volume fraction in liquid water*

The fully hydrated polymer volume fraction (ϕ_{2V}) was obtained from particle size determination in non-swelling and swelling states, as analogous to what was done previously (Mantovani et al., 2000). The size and distribution of each of the polymeric powders were measured by dynamic laser light scattering technique (Mastersizer®/E, Malvern Instruments Ltd., Worcestershire, UK). Alcohol and water were used as non-swelling and swelling media, respectively. ϕ_{2V} was obtained by comparing mean volume diameters according to the equation of $\phi_{2V} = [\overline{d_{al}}/\overline{d_w}]^3$, where $\overline{d_{al}}$ and $\overline{d_w}$ are geometric mean volume diameters of a powdered polymer in alcohol and in water, respectively.

To quantify the polymer volume fraction during ice-liquid phase transition of water denoted by φ_2, it was assumed that only pure water freezes when cooled to freezing point. φ_2 is thus directly proportional to the cumulative partial area under the DSC peak at corresponding T, i.e., $\varphi_2 = \varphi_2^{(i)} - \Lambda \frac{A_T}{P}$. Where, A_T, P, $\varphi_2^{(i)}$, and Λ are

the area under the peak at temperature T, the total area under the peak, the polymer volume fraction with water of fraction (i), and the linear coefficient that makes φ_2 equals φ_{2V} determined by light scattering technique, in which A_T equals P, respectively. $\varphi_2^{(i)}$ was approximated from mole fraction of water of fraction (i) ($x_1^{(i)}$) calculated based on the water content of non-freezable water previously described, i.e., $\varphi_2^{(i)} \approx (1 - x_1^{(i)})$. The φ_2 and its corresponding T were non-linearly fitted into Flory's model using the commercial software (SigmaPlot® 2000, SPSS, Inc.).

4. Results and Discussion

4.1 *In situ water crystallization: the validation of DSC measurement*

The cooling and heating traces revealing water crystallization and melting, respectively, are in Figure 1. There was an exothermic peak of water crystallization (I in Figure 1) occurred at a temperature far below zero °C. Endothermic melting peak (II in Figure 1), on the other hand, started at a normal melting temperature. This inconsistency between freezing and melting curves is commonly observed in fairly slow rate of scanning (1-10 °C/min). It is because the crystallization difficulty causes an exotherm to appear at a temperature lower than normal. It seems that the melting trace could approach an equilibrium ice-water transition better than cooling counterpart as the tracing was close to 0 °C. Table 1 shows the detailed information of water melting (II in Figure 1) compared with the reference (Dean, 1985).

As seen in Table 1, both onset and heat of melting for pure water agree with the values taken from the reference. Very low deviations, i.e., 0.37% and 1.18% deviate from reference values for onset and heat of melting, respectively, are observed. It has been stated that in typical DSC measurement, the mean error at heating/cooling rate of 1-10 °C/min should not exceed 2.5% (Borchard, et al., 2005).

Thus, the method and its conditions could be used to investigate water crystallization/melting with acceptable precision and accuracy.

4.2 *DSC water tracings in the selected hydrophilic polymers and the nature of ice-liquid water transition*

Figure 2 illustrates the tracings of water that could be found in SA, SSG, SCMC, and CCS equilibrated with ambient humidity (85-100% RH). For simplicity, the only tracings of SA-100%RH system are showed. As seen in Figure 2, the freezable water in current study is consistent with previous report (Nakamura et al., 1981). It is then subjected into 2 fractions, i.e., water of fraction (ii) labeled as (I) where freezing/melting happen at a temperature below zero, and that of fraction (iii) labeled as (II) where its transitions are closed to normal melting point. Figure 3 illustrates the DSC freezing traces of CCS with various aqueous level environments including that with liquid water in excess. It is noted that other polymers in this study showed similar patterns. However, the water transition tracings were absent in the cases of PS and HPMC in ambient humidity but fully hydrated samples. PS and HPMC are non-ionic polymers exhibiting less hygroscopic than others. It may be because ionic species and salts could attribute to hydration on polymer they present with and might allow amount of water uptake greater than threshold of non-frozen water to show the DSC tracings of water of fraction (ii) and (iii) in cases of SA, SSG, SCMC, and CCS.

Should the porosity formed by 3-dimentional polymer network govern the freezing/melting point depression, the depressed temperature in various moisture environments of the same polymer which would form similar pore structures might be invariant. Furthermore, if the pores collapse during ice formation, the transition of water of fraction (ii) might be either near or far from that of water of fraction (iii) dependent on the new size of the pores that water occupies after collapsing. As

obviously showed in Figures 3, there are not the cases in the present study. It is observed that the phase transition of water of fraction (ii) always exhibits a pattern as a polymer solution, i.e., the more concentration level of water; the more freezing temperature is depressed. Thus rather than porosity confinement, the freezing temperature may be depressed in accord with polymer-water interaction.

Figure 4 illustrates the endothermic melting traces of SSG with variety of humidity as well as fully hydrated sample. Like freezing exotherms, the melting endotherms of various level of water with polymer samples under study were also in similar patterns. It is observed that the melting of freezable bound water shifts toward the melting of free water. i.e., the two singlet peaks turn to a doublet with increase in water content which is similar to the previous study (Borchard et al., 2005). It may be because water of fraction (ii), during increasing temperature, becoming liquid phase migrates from the vicinity of polymer interaction sites within gel due to hydrogen bonding among water molecules to be in equilibrium again with free water that melt later at a normal melting temperature.

4.3 *Non-freezable bound water*

An attempt at the determination of water of fraction (i) for each of polymer-water systems was made and tabulated in Table 2. The materials under study exhibit the non-freezable water contents of between 9.67% and 26.63% whereas it was previously reported that starches and celluloses exhibited non-freezable bound water contents of 28% (Zhong & Sun, 2005) and 22-25% (Luukkonen, at al., 2001), respectively. McCrystal, et al (1997) estimated the number of moles of non-freezing water per a polymer repeating unit for HPMC gel as approximately 3.8 moles that is corresponding to approximately 10-20% water content dependent on degrees of substitution, while the current study on HPMC is within the range (13.21%, Table 2).

On the other hand, the cross-linked chemically modified starch and cellulose that are more hygroscopic (SSG and CCS) illustrate low level of non-freezable bound water (Table 2). It might be because these materials present more number of ice nuclei, during freezing, that draw more water molecules due to hydrogen bonding to the ice clusters as a process of lowering surface free energy. As a result more portion of freezable water may be detected.

4.4 *The volume fraction of polymeric hydrogels vs. melting depression: non-linear fitting to the Flory's model*

The volume fractions in liquid water ($\varphi_{2\,V}$'s) of fully hydrated polymers under study are tabulated in Table 2. It is noted that $\varphi_{2\,V}$'s of SA and HPMC have been taken from the reference (Mutalik, et al., 2006) since the polymers dissolved in water and alcohol, respectively. φ_{2V}'s of sodium starch glycolates have been previously reported as the numbers between 0.005 and 0.045 (Mantovani, et al., 2000) whereas $\varphi_{2\,V}$ of SSG which is chemically identical is 0.031 (Table 2). In addition, the DSC melting traces yield the endotherms closed to 0 °C compared to the exotherms of freezing traces (Figures 2 and 4). Thus the endothermic melting transition of a fully hydrated polymer is used in order to have an appropriate φ_2.

Each of φ_2-T data sets derived from DSC curves was non-linearly fitted into equation 4 with the restricted conditions that $(R/\Delta H_m) = 1.383 \times 10^{-3}$ K^{-1} and $T_0 =$ 273.15 K (Borchard, et al., 2005). The estimates as well as their standard errors (SE) of parameters including χ_1, network factor ($_{V_1}\frac{v_e}{V_0}$) and f are tabulated in Table 3. It is noted that ionic and/or cross-linking network contribution factor was set as null for uncharged and/or linear polymers, respectively. It was found that the model is successfully applied to φ_2-T data sets with high correlations (r^2: 0.934-0.999, Table 3). It is thus demonstrated that χ_1, charges, and polymer network affect the

crystallization/melting of water that the polymer contains. As see in Table 3, *f*'s of charged polymers are statistically significant from null at α-level of 0.05, so are network factors of cross-linked ones except CCS. *f* reflects the degree of ionization whereas network factor illustrates swelling of the cross-linked polymers (Borchard, et al., 2005; Mantovani, et al., 2000). It is observed that at 0.05-α-level, network factor in the case of CCS is not significantly different from null. It might evidently be because the swelling of the polymeric network is not sufficient to significantly effect on the water crystallization / melting for it was previously reported that the swelling capacity of CCS present in water was far lower than that of SSG (Visavarungroj & Remon, 1990). In addition, Okoroafor, et al. (1998) mentioned that the effect of network factor was quite small since its value usually is of the order of two decimal digits. That is consistent with the current study as it is observed that the estimates of network factor are in the same order of magnitude (Table 3).

4.5 *Flory's interaction parameter* (χ_1)

To characterize the thermodynamic interaction between water and polymer, Flory (1971) introduced a dimensionless quantity: χ_1. It represents merely the difference in energy divided by thermal agitation energy (kT: where k is Boltzmen's constant) of a solvent molecule immersed in the pure polymer compared with one surrounded by molecules of its own kind. A number of authors reported the magnitudes of χ_1 of aqueous polymeric solutions including starches and its derivatives (Baks, et al., 2007; Cruz-Orea, et al., 2002; Mantovani, et al., 2000; Farhat & Blanshard, 1997), and sodium alginate (Borchard, et al., 2005) as the numbers ranging between 0.43 and 0.67. As seen in Table 3, the estimates of χ_1-parameters of the same types of polymers vary between 0.520 and 0.761 which are comparable. Myagkova, et al. (1997) mentioned that the χ_1 should be approximately 0.5 for

maximum dissolving capacity of liquid water, i.e., the good-solvent conditions, for cellulose esters whereas the magnitudes of χ_1 for the same type of polymers under study are 0.679-0.847 which also approaches those conditions. In fact, the magnitude χ_1 is somewhat empirical and not a constant. It is dependent on volume fraction as well as temperature (Myagkova, et al.; 1997 and Flory, 1971). Thus experimental conditions should affect its magnitude especially during the initial setting causing χ_1 values to deviate from laboratories to laboratories.

Figure 5 illustrates the plot of χ_1 versus the reciprocal absolute temperature of the onset of DSC melting transition of water of fraction (ii) in fully hydrated samples. It is observed that the smaller the value of χ_1, the larger solvent water melting was depressed, i.e., stronger affinity for water. Flory (1971) rectified the energy quantity of χ_1 that should be regarded as the free energy change rather than as the heat of mixing only. χ_1 then contains an entropy contribution in addition to enthalpy one. Thus, in a simple case (Borchard, et al., 2005):

$$\chi_1 = \alpha_1 + \frac{\beta_1}{T} \quad (4)$$

where, α_1 and β_1 are entropy and enthalpy parameters, respectively. Assuming the same type of interaction, χ_1 derived from polymeric hydrogels in this study could exhibit the relationship with $1/T$ as showed by Equation 4. As seen in Figure 5, the trend line as well as 95% confidence interval (dotted lines in Figure 5) represents the data fitting of Equation 4. Unfortunately, the power of regression and the correlation coefficient are as low as 25.01% and 0.631, respectively. It might be because the variety in nature of individual polymers and experimental conditions could complicate the systems resulting the fitted parameters are so empirical that they are meaningless to address.

Acknowledgement

The authors would like to thank Thailand Research Fund for financial support.

Special thanks also go to the Scientific Equipment Center, Prince of Songkla University; Faculty of Pharmaceutical Sciences' Research and Development Unit; and the Department of Pharmaceutical Technology, Faculty of Pharmaceutical Sciences, Prince of Songkla University for providing the lab facilities.

References

Baks, T., Ngene, I. S., van Soest, J. J. G., Janssen, A. E. M., Boom, R. M. 2007. Comparison of methods to determine the degree of gelatinisation for both high and low starch concentrations. *Carbohyd. Polym*. 67: 481-490.

Borchard, W., Kenning, A., Kapp, A., Mayer, C. 2005. Phase diagram of the system sodium alginate/water: A model for biofilms. *Int. J. Biol. Macromole*. 35: 247-256.

Dean, J. A., 1985. Lange's Handbook of chemistry, 13rd Ed., McGraw-Hill, New York, p. 9-117.

Faroongsarng, D., Peck, G. E. 2003. Thermal porosity analysis of croscarmellose sodium and sodium Starch Glycolate by differential scanning calorimetry. *AAPSPharmSciTech*. 4(4): article 67.

Flory, P. J. 1971. *Principles of polymer chemistry*. Cornell University Press, Ithaca and London.

Hay, J. N., Laity, P. R. 2000. Observation of water migration during thermoporometry studies of cellulose films. *Polymer*. 41: 6171-6180.

Higuchi, A., Iijima, T. 1985. DSC investigation of the states of the water in poly(vinyl alcohol) membranes. *Polymer*. 26: 1207-1211

Ilmain, F., Tanaka, T., Kokufuta, E. 1991. Volume transition in a gel driven by hydrogen bonding. *Nature*. 349: 400-401.

Ishikiriyama, K., Todoki, M. 1995. Pore size distribution measurements of silica gels by means of differential scanning calorimetry. *J. Colloid Interf. Sci.* 171: 103-111.

Luukkonen, P., Maloney, T., Rantanen, J., Paulapuro, H., Yliruusi, J. 2001. Microcrystalline cellulose-water interaction-A novel approach using thermoporosimetry. *Pharm. Res*. 18(11): 1562-1569.

Mantovani, F., Grassi, M., Colombo, I., Lapasin, R. 2000. A combination of vapor sorption and dynamic laser light scattering methods for the determination of the parameter χ and the crosslimk density of a powdered polymeric gel. *Fluid Phase Equilibr*. 167: 63-81.

McCrystal, C. B, Ford, J. L., Rajabi-Siahboomi, A. R. 1997. A study on the interaction of water and cellulose ethers using differential scanning calorimetry. *Thermochim. Acta*. 294: 91-98.

Mutalik, V., Manjeshwar, L. S., Wali, A., Sairam, M., Raju, K. V. S. N., Aminabhavi, T. M. 2006. Thermodynamics/hydrodymanics of aqueous polymer solutions and dynamic mechanical characterization of solid films of chitosan, sodium alginate, guar gum, hydroxyl ethyl cellulose and hydroxypropyl methylcellulose at different temperatures. *Carbohyd. Polym*. 65: 9-21.

Myagkova, N. V., Rakhmonberdiev, G. R., Sagdieva, Z. G., Sidikov, A. S. 1997. Thermodynamic properties of solutions of water-soluble mixed cellulose esters. *Chem. Nat. Compd*. 33(1): 76-79.

Nakamura, K., Hatakeyama, T., Hatakeyama, H. 1981. Studies on bound water of cellulose by differential scanning calorimetry. *Tex. Res. J*. 51(9): 607-613.

Okoroafor, E. U., Newborough, M., Highgate, D., Augood, P. 1998. The thermal behaviour of water in crosslinked hydro-active polymeric structure: crystasllization of water. *J. Phys. D: Appl. Phys*. 31: 3120-3129.

Ozmen, M. M., Okay, O. 2005. *Polymer*. 46: 8119-8127.

Ping, Z. H., Nguyen, Q. T., Chen, S.M., Zhou, J. Q., Ding, Y. D. 2001. States of water in different hydrophilic polymers-DSC and FTIR studies. *Polymer*. 42: 8461-8467.

Rajabi-Siahboomi, A. R., Bowtell, R. W., Mansfield, P., Davies, M. C., Melia, C. D. 1996. Structure and Behavior in Hydrophilic Matrix Sustained Release Dosage Forms: 4. Studies of Water Mobility and Diffusion Coefficients in the Gel Layer of HPMC Tablets Using NMR Imaging. *Pharm Res*. 13(3): 376-380.

Rault, J., Gref, R., Ping, Z. H., Nguyen, Q. T., Neel, J. 1995. *Polymer*. 36: 1655-31.

Visavarungroj N, Remon J P. 1990. Crosslinked starch as a disintegrating agent. *Int. J. Pharm*. 62: 125-131.

Yamamoto, T., Mukai, S.R., Nitta, K., Tamon, H., Endo, A., Ohmori, T., Nakaiwa, M. 2005. Evaluation of porous structure of resorcinol-formaldehyde hydrogels by thermoporometry. *Thermochim. acta*. 439: 74-79.

Zhong, Z., Sun, X. S. 2005. Thermal characterization and phase behavior of cornstarch studied by differential scanning calorimetry. *J. Food Eng*. 69: 453-459.

Zografi, G., Kontny, M. J. 1986. The interactions of water with cellulose- and starch-derived pharmaceutical excipients. *Pharm. Res*. 3(4): 187-194.

Parameter	DSC run	Reference (1)	Deviation (%)
Onset; Peak (K)	274.15; 275.4	273.15	+0.37; +0.82
Heat of melting (Kcal/mol)	1.453	1.436	+1.18

Table 1.Water melting information taken from endotherm (heating trace) compared with the reference (Dean, 1985).

Polymeric material	[1]Overall water content (%)	[2]Freezable water content (%) (mean, s.d.)	[3]Water of fraction (i) (%)	[4] φ_{2V}
PS	80.01	53.38, 1.09	26.63	0.112
SA	73.36	47.43, 1.07	25.93	[a]0.167
SSG	73.28	52.30, 1.11	20.98	0.031
HPMC	51.30	38.09, 0.87	13.21	[a]0.384
SCMC	69.13	46.14, 0.78	22.99	0.145
CCS	79.97	70.30, 1.11	9.67	0.054

1. Overall water content was determined by moisture balance.
2. Freezable water content was determined by DSC traces calculation (in 3 replicates) based on the heat of melting in Table 1.
3. Non-freezable water content was calculated as Overall water content minus Freezable water content.
4. The fully hydrated polymer volume fraction based on equation (Mantovani et al., 2000): $\phi_{2V} = [\overline{d_{al}}/\overline{d_w}]^3$ where $\overline{d_{al}}$ and $\overline{d_w}$ are geometric mean volume diameters of a powdered polymer in alcohol and in water, respectively.

a. The numbers are taken from reference (Mutalik et al., 2006) since the equipment could not determine.

Table 2. Water contents and the volume fractions of fully hydrated hydrophilic polymers under study.

Polymeric material	χ_1 Estimate, SE	$V_1\frac{v_e}{V_0}$ Estimate, SE	f Estimate, SE	r^2
PS	0.761, 0.041	0.067, 0.017	**-	0.939
SA	0.738, 0.033	*-	0.513, 0.022	0.986
SSG	0.520, 0.051	0.084, 0.010	0.288, 0.093	0.994
HPMC	0.847, 0.032	*-	**-	0.934
SCMC	0.776, 0.021	*-	0.368, 0.070	0.947
CCS	0.679, 0.025	[a] 0.028, 0.048	0.241, 0.002	0.999

* Since the polymers are linear, network contribution is absent.
**Since the polymers are uncharged, the reduced model with $f = 0$ is used.
[a] The contribution is statistically non-significant at 0.05 α-level.

Table 3. The estimates of the parameters according to the restricted ($R/\Delta H_m = 1.383 \times 10^{-3}$ K^{-1} and $T_0 = 273.15$ K) non-linear regression of equation 3.

Figure legends

Figure 1. DSC thermograms of water illustrating water crystallization (cooling trace: I) and melting (heating trace: II). DSC was done according to the conditions listed in Table 1.

Figure 2. DSC thermograms (cooling [A] and heating [B] curves) of SA previously equilibrated in 100%RH at 30 degrees C for 7 days showing 2 phases of water on a polymer surface. (I) is freezable bound water and (II) is bulk water.

Figure 3. DSC freezing traces of water in the samples of CCS equilibrated with (a) 96% RH, (b) 100%RH, and (c) liquid water. It is noted that hydrogels of other polymer under study also exhibit similar behavior.

Figure 4. DSC endothermic melting of ice in SSG equilibrated with (a) 84% RH, (b) 96% RH, (c) 100% RH, and (d) excess liquid water (fully hydrated). It is noted that hydrogels of other polymer under study also exhibit similar behavior.

Figure 5. The plot of χ_1-parameter against the reciprocal of onset temperature (in absolute scale) of melting transition of freezable bound water in water-polymer systems under study.

Figure 1
Click here to download high resolution image

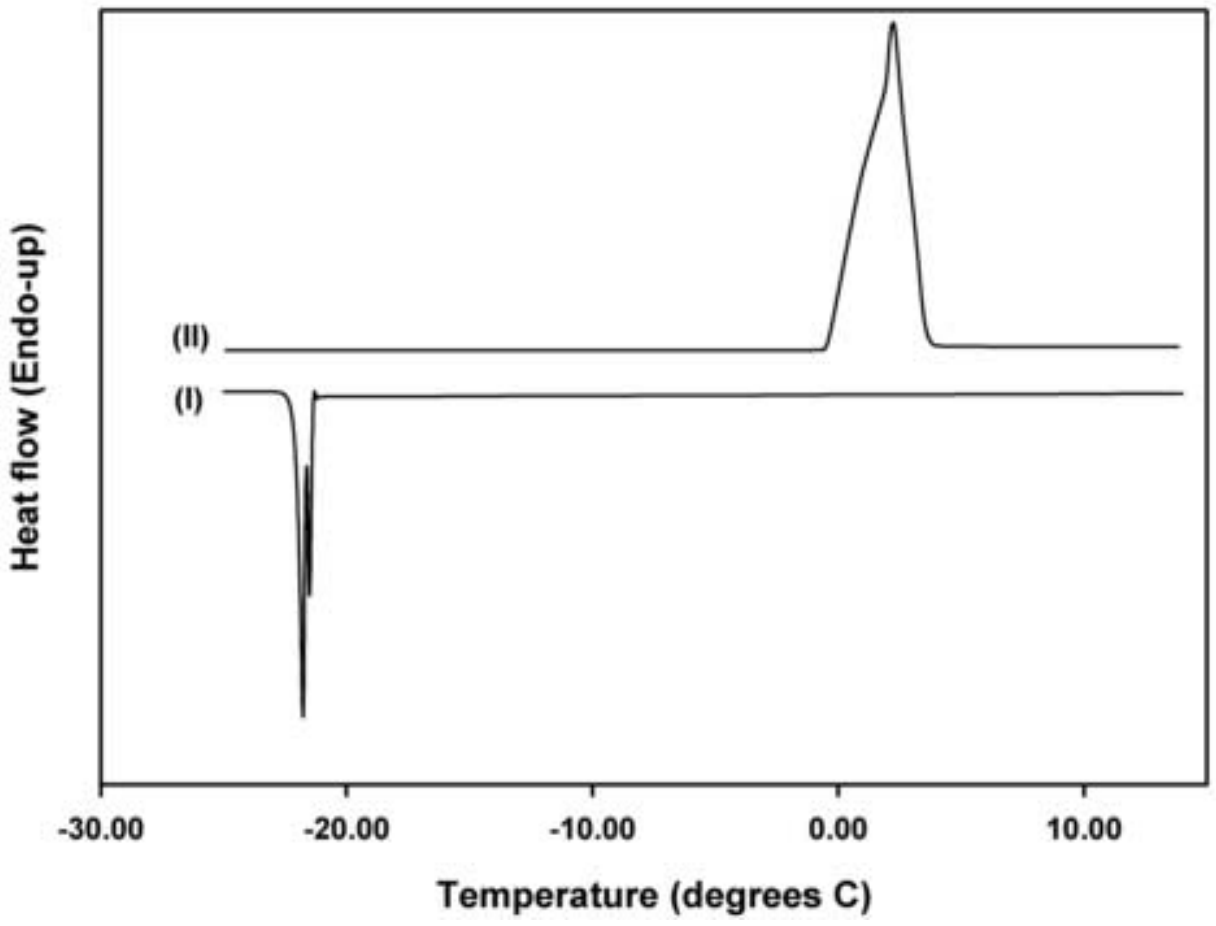

Figure 2
Click here to download high resolution image

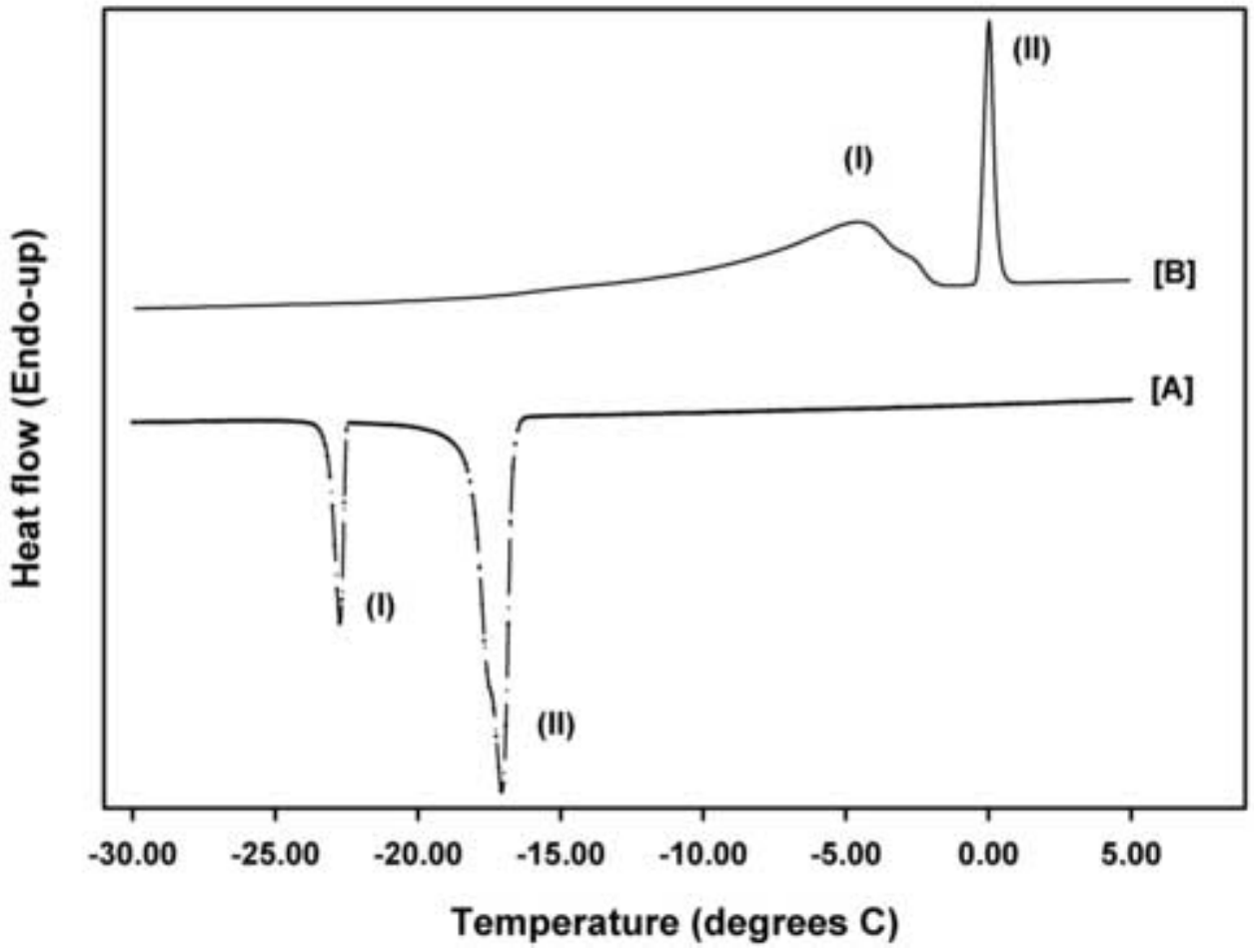

Figure 3
Click here to download high resolution image

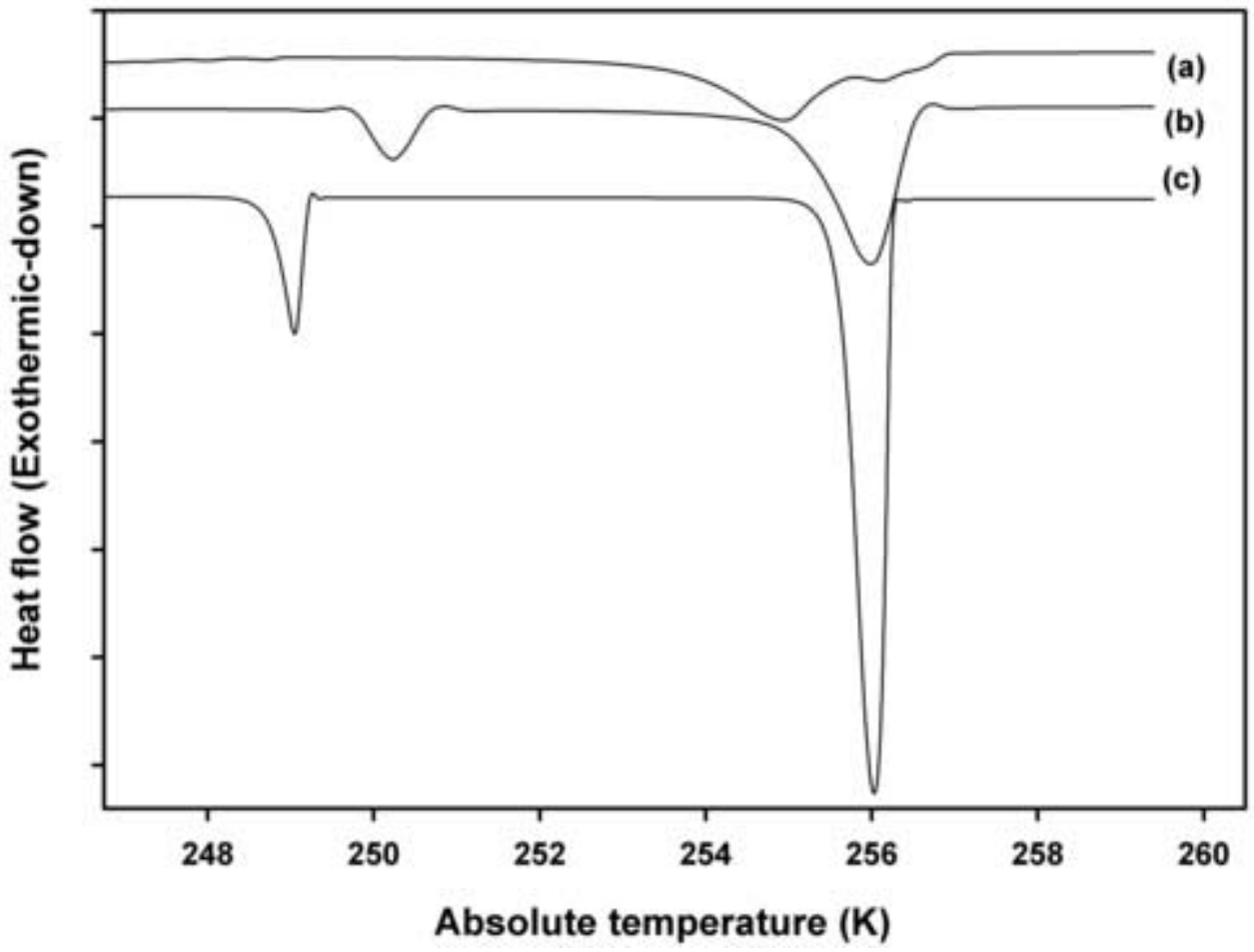

Figure 4
Click here to download high resolution image

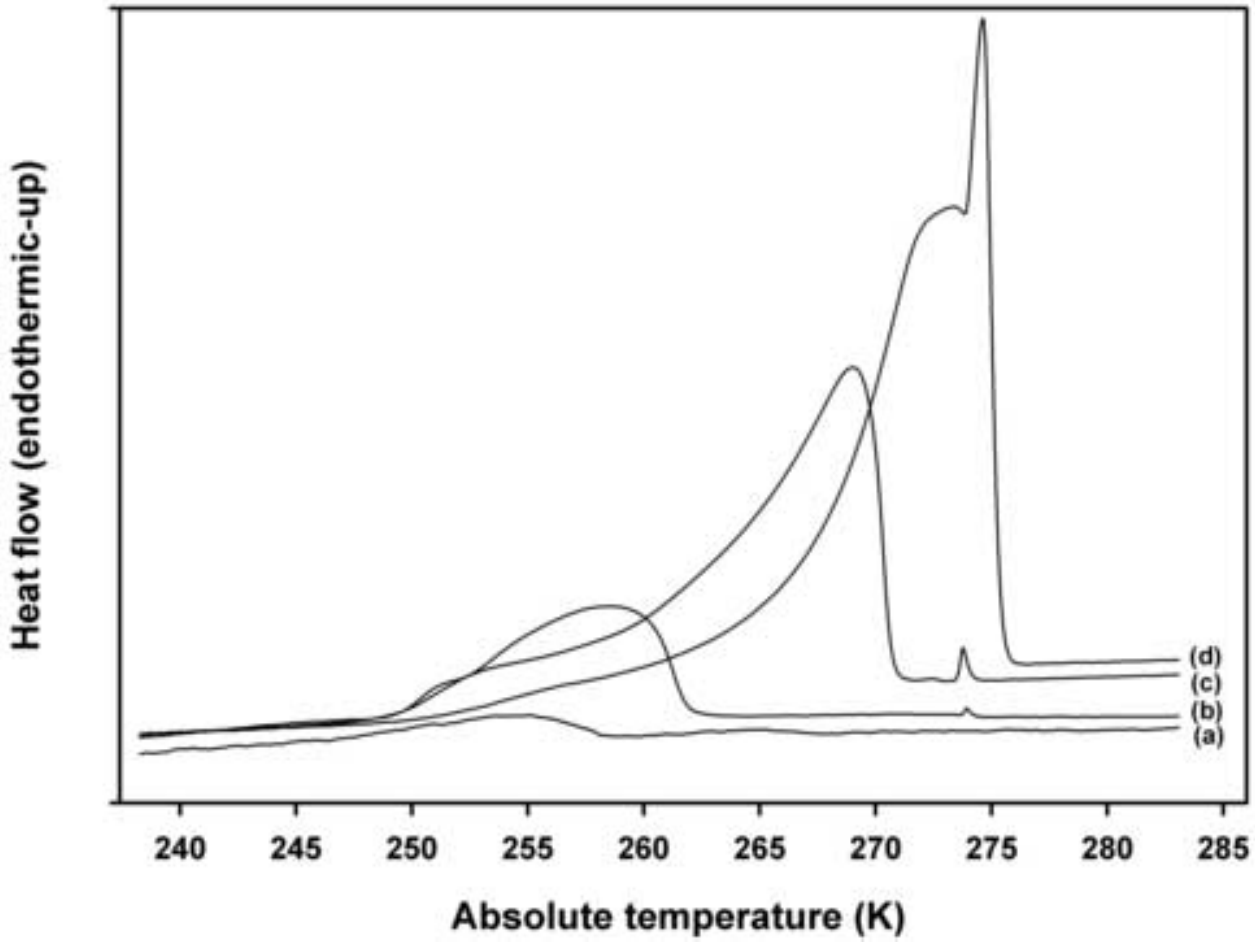

Figure 5
Click here to download high resolution image